Approaches to Suppress CO?-Induced Plasticization of Polyimide Membranes in Gas Separation Applications

Authors:

Moli Zhang, Liming Deng, Dongxiao Xiang, Bing Cao, Seyed Saeid Hosseini, Pei Li

Abstract:

Polyimides with excellent physicochemical properties have aroused a great deal of interest as gas separation membranes; however, the severe performance decay due to CO?-induced plasticization remains a challenge. Fortunately, in recent years, advanced plasticization-resistant membranes of great commercial and environmental relevance have been developed. In this review, we investigate the mechanism of plasticization due to CO? permeation, introduce effective methods to suppress CO?-induced plasticization, propose evaluation criteria to assess the reduced plasticization performance, and clarify typical methods used for designing anti-plasticization membranes.

Approaches to Suppress CO$_2$-Induced Plasticization of Polyimide Membranes in Gas Separation Applications

Moli Zhang [1], Liming Deng [1], Dongxiao Xiang [1], Bing Cao [1], Seyed Saeid Hosseini [2,* and Pei Li [1,*

[1] College of Materials Science and Engineering, Beijing University of Chemical Technology, Beijing 100029, China; mollyzhang6@163.com (M.Z.); dlm0517@163.com (L.D.); xdx_xiang@163.com (D.X.); bcao@mail.buct.edu.cn (B.C.)

[2] Membrane Science and Technology Research Group, Department of Chemical Engineering, Tarbiat Modares University, Tehran 14115, Iran

* Correspondence: saeid.hosseini@modares.ac.ir (S.S.H.); lipei@mail.buct.edu.cn (P.L.); Tel.: 86-10-6441-3857 (S.S.H. & P.L.)

Abstract: Polyimides with excellent physicochemical properties have aroused a great deal of interest as gas separation membranes; however, the severe performance decay due to CO$_2$-induced plasticization remains a challenge. Fortunately, in recent years, advanced plasticization-resistant membranes of great commercial and environmental relevance have been developed. In this review, we investigate the mechanism of plasticization due to CO$_2$ permeation, introduce effective methods to suppress CO$_2$-induced plasticization, propose evaluation criteria to assess the reduced plasticization performance, and clarify typical methods used for designing anti-plasticization membranes.

Keywords: polyimide; plasticization; membrane; gas separation; carbon dioxide
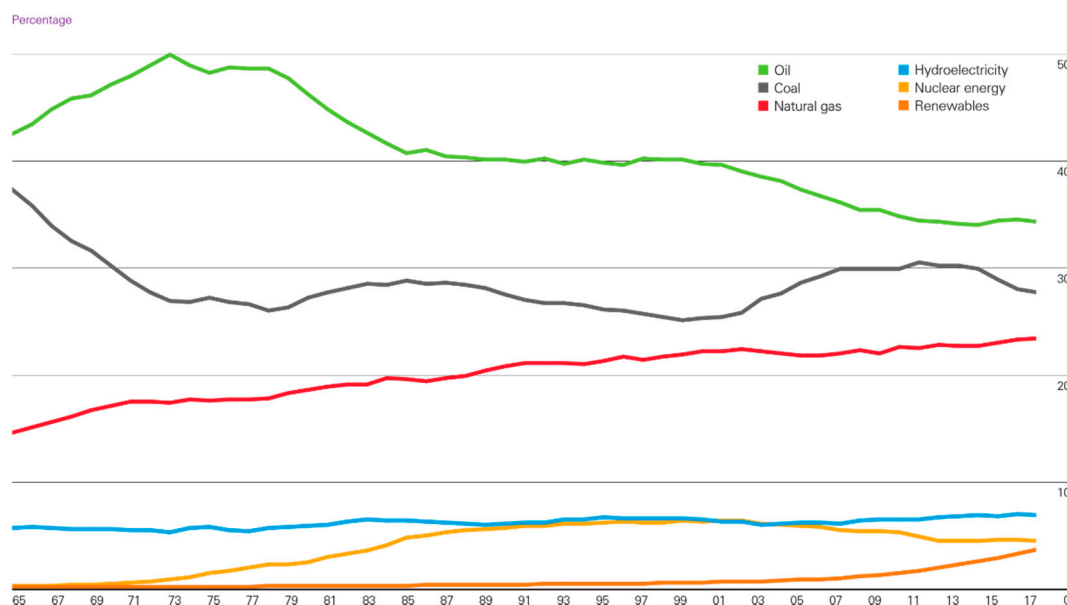
1. Introduction

1.1. Natural Gas Process

Narrowly speaking, natural gas—a term in the energy field—is referred to as a mixture of hydrocarbons and non-hydrocarbon gases that naturally exist underground. The typical composition of raw natural gas is shown in Table 1, based on samples from eight different locations worldwide [1,2]. Methane is the main component of raw natural gas—one of the raw materials. It is consumed during combustion for heat release or chemical production. When producing the same amount of energy, CO$_2$ emissions by natural gas are ~26% less than oil and coal [3]. Therefore, natural gas is regarded as a source for the cleanest and lowest carbon emitting fossil fuel in the world [4].

Table 1. Typical composition of raw natural gas [1,2].

Component	Composition Range (mol%)
CH_4	29.98–90.12
C_2H_6	0.55–14.22
C_3H_8	0.23–12.54
C_4H_{10}	0.14–8.12
C_{5+}	0.037–3.0
N_2	0.21–26.10
H_2S	0.0–3.3
CO_2	0.06–42.66
He	0.0–1.8

According to the BP (British Petroleum) Statistical Review of World Energy (2018), 2017 witnessed the fastest rates of rapid increases in natural gas consumption (3.0%; 96 billion cubic meters) and production (4.0%; 131 billion cubic meters) [5]. Furthermore, Figure 1 clearly illustrates that in 2017, the share of natural gas in global primary energy consumption by fuel consistently increased to 23.4% [6]. Undoubtedly, strong natural gas growth can be expected in the near future. This is supported by an increase in the levels of industrialization and power demand, continued coal-to-gas switching, and the growing availability of low-cost supplies [7]. In conclusion, the rapid increase in natural gas consumption has driven the necessity for natural gas processing to meet pipeline requirements.

Figure 1. Shares of global primary energy consumption by fuel [6].

It has been widely recognized that variations in raw natural gas consumption are considerably region-dependent [8], which is supported by the worldwide composition data of raw natural gas (shown in Table 2). Nevertheless, nations tightly control the composition of natural gas prior to entry into the industrial pipeline grids. Take the U.S. for example, where Table 3 shows a whole set of criteria defining the upper limits of common impurities. Therefore, to remove the undesired components and ultimately meet the requirements of target composition specifications, preconditioning is required for all raw natural gases. Furthermore, the greenhouse effect generated by CH_4 must also be taken into consideration. Generally speaking, if CH_4 is released during the purification and shipment of natural gas, it may cause a severe greenhouse effect.

Table 2. Composition of natural gas reservoirs (volume percent) in some regions of the world [9].

Component	Groningen (Netherlands)	Laeq (France)	Uch (Pakistan)	Uthmaniyah (Saudi Arabia)	Ardjuna (Indonesia)
CH_4	81.3	69	27.3	55.5	65.7
C_2H_6	2.9	3	0.7	18	8.5
C_3H_8	0.4	0.9	0.3	9.8	14.5
C_4H_{10}	0.1	0.5	0.3	4.5	5.1
C_{5+}	0.1	0.5	-	1.6	0.8
N_2	14.3	1.5	25.2	0.2	1.3
H_2S	-	15.3	-	1.5	-
CO_2	0.9	9.3	46.2	8.9	4.1

Table 3. Composition specifications for natural gas delivery to the U.S. national pipeline grid [10].

Component	Specification
CO_2	<2%
H_2O	<120 ppm
H_2S	<4 ppm
C_3+ content	950–1050 Btu/scf; dew point: $<-20\,°C$
total inert gases (N_2, He)	<4%

Notes: ppm, parts per million; and scf, standard cubic feet.

CO_2 can reduce the calorific value of natural gas and result in global warming. CO_2 and H_2S contribute to the corrosion of natural gas pipelines; therefore, numerous studies have been conducted to remove such acidic gases [11,12]. The most extensively used methods include cryogenic distillation [13,14], amine absorption [15], pressure swing adsorption (PSA) [16,17], and membrane separation technologies. Of these, cryogenic distillation requires a large amount of energy to condense permanent gases such as CO_2 [16]. Therefore, a hybrid system combining amine absorption with membrane separation is preferred due to its high energy efficiency [18].

The amine absorption process has displayed favorable performance in extracting CO_2 from the CO_2/CH_4 gas mixtures. However, the high capital and operating costs remain a problem. Membrane technology is a good alternative for gas separation, ascribed to its low capital investment and ease of operation. It also exhibits the efficiency of the membrane units, and advantages of design flexibility and compactness [19]. This technology is expected to be the superior gas separation method when CO_2/CH_4 selectivity is increased to 40 [20]. However, the presence of CO_2 and/or other highly sorbing components can result in membrane plasticization and swelling.
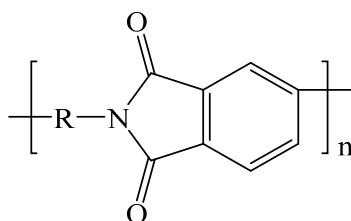
1.2. Membrane Materials Used for Gas Separation

Progress in membrane technology has been largely dependent on high-performance membrane materials. Inorganic membranes are not discussed in this paper due to their expensive module fabrication and limited industrial applications, even though considerable progress has been achieved in this field. This review focuses on polymer membranes. To date, a variety of promising polymer membranes, including cellulose acetate (CA) [21,22], polycarbonate (PC) [23–27], polysulfone (PSF) [28–30], polymethyl methacrylate (PMMA) [31–33], polyimide (PI), and polymer of intrinsic microporosity (PIMs) [34–37], have been developed to meet the demands of the gas separation industry.

There are many promising polymer membrane materials, yet the gas separation market is only dominated by a few. This can be explained by the different operating conditions between research laboratories and industrial applications. Current commercial membranes are used under high pressure, and high concentrations of plasticizing impurities such as water, BTEX aromatics (The term "BTEX aromatics" refers to benzene, toluene, ethylbenzene, and xylene), and other heavy hydrocarbons [10]. Performance stability, chemical resistance, and low capital cost should also be incorporated into the criteria of producing industrially available membranes [20].

In particular, cellulose acetate, polyimides and perfluoropolymers are commercially available polymers used for fabricating CO_2 removal membranes [10]. The performance of CA-based membranes, and a range of polyimide membranes, have been summarized in detail by Scholes et al. [38] and will not be discussed in this review.

Throughout this paper, the term polyimide represents aromatic polyimide. Aromatic polyimides contain the imide group—a constitutional unit in the polymer backbone (illustrated in Figure 2). It is a linear and heterocyclic aromatic polymer, widely used to synthesize films, fibers, molding powders, coatings, and composites. Its outstanding heat resistance, relatively high resistance to chemical solvents, strong mechanical strength, and high selectivity in major gas pairs (such as CO_2/CH_4 and O_2/N_2), make polyimide an attractive candidate amid many polymeric membranes. Since the manufacture of commercial polyimides membranes, many have been developed for gas separation, and used in the separation process by the DuPont (USA) and Ube (Japan) industries [39].

Figure 2. Chemical structure of polyimides.

Strong plasticization resistance is required in several gas separation applications such as CO_2/CH_4, propylene/propane, and butadiene/butane separations, which can be attributed to the presence of highly sorbing components. The CO_2/CH_4 separation containing CO_2 sorbates, is more frequently encountered in industrial applications such as high-pressure natural gas sweetening and enhanced oil recovery (EOR). Hence, there is a growing concern over the development of polyimide membranes with a reduced plasticization effect and minimal loss of selectivity. Numerous studies over the past decade have been carried out to investigate the mechanisms and suppression methods of plasticization [40].

1.3. Plasticization in Polyimides

Plasticization is usually defined as the increased segmentation mobility of polymer chains [41]. CO_2 permeability will rise with increased feed pressure after a critical point, which is generally regarded as the mark of being plasticized. Simultaneously, an undesired loss of gas pair selectivity is often observed. Under the high pressure of CO_2, the polymer matrix swells, subsequently resulting in possible free volume changes and inter-chain spacing. Consequently, the mobility of the polymer segments increases, thus weakening the size-sieving ability of polyimide membranes. The plasticization phenomena can be demonstrated by the obvious loss of selectivity. Therefore, developing membrane materials that can maintain gas selectivity in the presence of aggressive feed streams is of utmost importance.

Some intriguing methods for prominently improving the plasticization resistance of polyimide membranes are illustrated in this article. Among them, crosslinking, such as thermal crosslink, diamine crosslink, diol crosslink, semi-interpenetrating networks, ultraviolet (UV) crosslink, and hydrogen bonding, is a practical and widely used method described in the literature. Furthermore, mixed matrix membranes (MMMs) or polymer blending have also been proposed to resist plasticization.
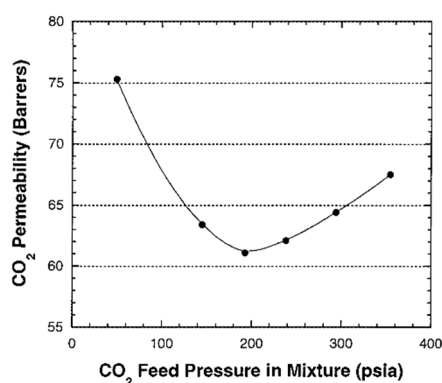
This review mainly focuses on approaches to suppress the notorious CO_2-induced plasticization of polyimide membranes. Furthermore, the mechanism, attractive advantages, and unavoidable weakness of each method are specified in the corresponding sections and illustrated in some cited literature. Some recent achievements and representative work are discussed in detail. It is fundamental to understand plasticization mechanisms and principles in order to design polyimide membranes with

less plasticization effect. In the end, a promising prospect is provided to instruct further research and propose some constructive suggestions.

2. Plasticization Mechanism

Plasticization often takes place in the presence of highly condensable gases (such as CO_2), especially under aggressive conditions (like high pressure and low temperature). There have been numerous studies on plasticization during the separation process of mixed gases such as CO_2/CH_4, propylene/propane [42–46], and ethylene/ethane [47,48]. This review mainly focuses on the CO_2-induced plasticization phenomenon, which usually happens during the natural gas sweetening process where CO_2 acts as a plasticizer.

Plasticization can be observed through multiple measures. The most commonly used approach is monitoring CO_2 permeability while increasing CO_2 feed pressure to observe the changes in polymer chain segmental mobility. During the gas permeation process, CO_2 permeability coefficients of most glassy polyimides will descend first due to the saturation of Langmuir sites. The polymer matrix will swell when CO_2 concentrations reach a critical point. Then, an obvious acceleration in gas permeability is observed with increasing CO_2 partial pressure [49] (Figure 3 [41]). Feed pressure at the minimum point of a CO_2 permeability curve is commonly defined as the plasticization pressure, which is an important indicator of plasticization. Simultaneously, a loss in gas pair selectivity occurs.

Figure 3. Mixed gas separation characteristics for 6FDA-6FpDA using 50:50 CO_2/CH_4 mixtures at 35 °C [41]. Notes: 6FDA, 4,4′-(hexafluoroisopropylidene)diphthalic anhydride; and 6FpDA, 4,4′-(9-fluorenylidene) bis (2-methyl-6-isopropylaniline).

Changes in the physical properties of membranes such as glass transition temperature (T_g), membrane thickness, and refractive index, can also indicate plasticization [50]. However, the occurrence of one sign is not necessarily accompanied by changes in other chemical or physical properties. In the case of polyethersulfone (PES), for example, although the decreased CO_2/CH_4 selectivity indicates that the polymer is plasticized, CO_2 permeability at 25 °C decreases by 54% as the CO_2 feed pressure increases from 0 to 27 atm [51]. This indicates that polymer matrix plasticization will not necessarily lead to an increase in permeability of all gases.

The polymer matrix can absorb a certain amount of CO_2 at modest pressure, leading to a significant reduction in the glass transition temperature [52]. In the range of low pressure, decrease in the permeability coefficient with increasing partial pressure is caused by the diminution of the solubility coefficient. In the range of high pressure, the positive correlation between the permeability coefficient and partial pressure is typical plasticizing behavior, which cannot be described by the dual mode mobility model [53].

After a systematic study of the plasticizing phenomena caused by CO_2 in 11 different glassy polymers, Bos et al. believed that the plasticization of a glass polymer could be defined as a function of the increase in the CO_2 permeability coefficient to the pressure of the feed gas, and the minimum pressure required to increase the permeability coefficient was defined as the plasticizing pressure [54].

It is generally believed that the diffusion coefficient increases when CO_2 concentrations exceed the critical value required by plasticization (namely, when the feed pressure exceeds the plasticizing pressure), subsequently leading to the increment of the permeability coefficient [55]. For glass polymers, the plasticization phenomenon occurs when polymer CO_2 concentrations reach critical levels. However, the critical pressure is polymer-dependent. Plasticization pressures of different polyimide membranes reported in the literature are listed in Table 4.

Plasticization induces chain relaxation and results in increased diffusivity of all gases in the feed mixture. Therefore, the reduction in membrane selectivity can be observed. A plasticization problem is that it can be inhibited by limiting the flexibility of polymer segments. There are many approaches that are currently being used to inhibit polymer segment flexibility, which are critically discussed in the subsequent sections.

Table 4. Different plasticization pressures reported in the literature.

CL Method	SU-1 or BC-1	SU-2 or BC-2	SU-3 or BC-3	Crosslinker or Fillers	Plasticization Pressure (atm)	Ref.
Decarboxylation CL	6FDA	DAM	DABA	-	~34.02	[56]
Decarboxylation CL	6FDA	DAM	DABA	-	-	[57]
Decarboxylation CL	6FDA	CADA1 /CADA2	BTDA /DSDA	-	30	[58]
Decarboxylation CL	6FDA	MPP	PP	-	30.62	[59]
Decarboxylation CL	6FDA	DAT	DATCA	-	30	[60]
Heat at 350 °C	Matrimid	-	-	-	>39.48	[61]
TR	-	-	-	-	20 (partial pressure)	[62]
TR	6FDA	HAB	-	-	>25 (fugacity)	[63]
Diamino	6FDA	durene	-	EDA	48.99	[64]
Diamino	6FDA	durene	-	CHBA	48.99	[65]
Diamino	6FDA	durene	-	PAMAM/DAB	30	[66]
Diamino	6FDA	Matrimid	-	p-xylenediamine	>32	[67]
Diol	6FDA	*m*PD	DABA	EG	35	[19]
Diol	6FDA	6FpDA	DABA	EG	-	[41]
Diol	6FDA	DAM	DABA	CHDM	-	[68]
Diol	6FDA	DAM	DABA	EG/CHDM	40	[69]
Semi-IPN	Matrimid	-	-	Thermid FA-700	>49.35	[70]
Semi-IPN	Matrimid	-	-	DCFT	>30	[71]
Semi-IPN	6FDA	NDA	TMPDA	azide	30	[72]
Ionic	6FDA	durene	-	N,N′-dimethylpiperazine	25	[73]
MMMs	6FDA	durene	DABA	ZIF-8	30	[74]
MMMs	*w*-PS	-	-	ZIF-8	-	[75]
MMMs	6FDA	durene	-	zeolite T	19.74	[76]
MMMs	Matrimid	-	-	MIL-53(Al) ZIF-8 Cu$_3$BTC$_2$	-	[77]
MMMs	Matrimid 6FDA	DAT durene	DAM	Ni$_2$(dobdc)	-	[78]
Blending	Matrimid	PSF	-	-	35	[79]
Blending	Matrimid	P84	-	-	14.80	[80]
Blending	Matrimid	cPIM-1	-	-	20	[81]
Blending	Torlon	cPIM-1	-	-	30	[82]

In this table: CL, crosslink; SU, structure unit; BC, blending component; TR, thermal rearrangement; DAM, 2,4,6-trimethyl-1,3-phenylenediamine; DABA, 3,5-diaminobenzoic acid; CADA1, carboxylic acid-containing diamine with -CF$_3$ group; CADA2, carboxylic acid-containing diamine with -H group; BTDA, 3,3′,4,4′-benzophenonetetracarboxylic dianhydride; DSDA, 3,3′,4,4′-diphenylsulfonetetracarboxylic dianhydride; MPP, 3,3-bis[4-(4-amino-3-methylphenoxy)phenyl]phthalide; PP, 3,3-bis[4-(4-aminophenoxy)phenyl]phthalide; DAT, 2,6-diaminotriptycene; DATCA, 2,6-diaminotriptycene-14-carboxylic acid; HAB, 3,3′-dihydroxy-4,4′-diamino-biphenyl; EDA, 1,2-ethylene diamine; CHBA, 1,3-cyclohexanebis (methylamine); PAMAM, polyamidoamine; DAB, diaminobutane; *m*PD, *m*-phenylene diamine; EG, ethylene glycol; CHDM, cyclohexane-1,4-diyldimethanol; DCFT, phenolphthalein dicyanate; NDA, 1,5-naphthalenediamine; TMPDA, 2,3,5,6-tetramethyl-1,4-phenylenediamine; ZIF-8, zeolite imidazole framework-8; *w*-PS, waste polystyrene; MIL-53(Al), aluminum terephthalate; Cu$_3$BTC$_2$, copper benzene-1,3,5-tricarboxylate; PSF, polysulfone; and cPIM-1, carboxylated polymer of intrinsic microporosity-1.

3. Methods to Reduce CO$_2$-Induced Plasticization

Extensive studies have been carried out and have successfully achieved suppression of polyimide membrane plasticization. Many criteria are available to classify these approaches, which are considerably involved in the formation of crosslink networks. Some crosslink networks are formed firmly by physical bonds such as hydrogen bonds, while others are formed by chemical bonds. A wide range of methods can achieve chemical bonds of polymer chains such as thermal treatment, chemical crosslinking using diamine or diol, formation of semi-interpenetrating networks, and UV crosslinking. Crosslinking is a practical and widely used approach to inhibit the plasticization of membrane materials. Some typical technologies of crosslinking are introduced in the following sections.

3.1. Thermal-Induced Crosslink

Rapidly quenching polyimide polymers can significantly suppress undesirable plasticization and introduce excess free volume into the polyimide matrix, thereby leading to greater stabilization in typical solvents. To illustrate, aromatic carboxylic acids along backbones can be dehydrated to form anhydride, which is subsequently decomposed into aryl radicals. A hydrogen atom will be abstracted from the backbone to bond covalently with the aryl radical, which is likely to occur in specific reactive sites.
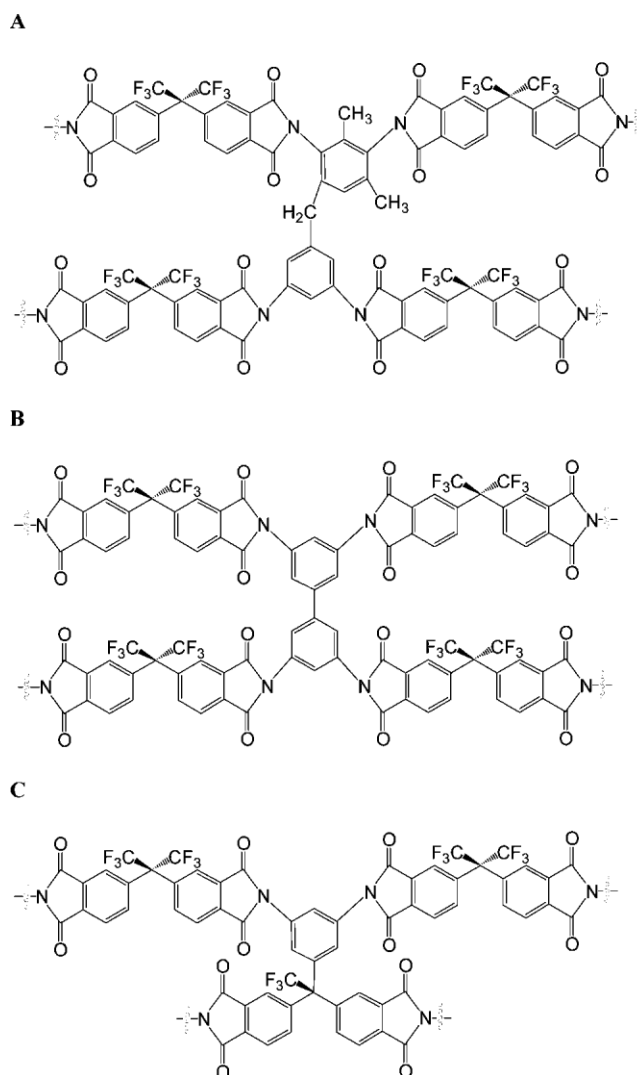
Steric hindrance of both functional and pendant groups must be taken into consideration while designing the crosslink points, since some structures (such as –CF$_3$) are too large for steric reactivity. Fine-tuning crosslink networks is not possible using this method, because the sites and extent of the crosslink are not measurable or quantifiable as a result of the non-definitive and insufficiently understood mechanism.

Matrimid 5218 has been utilized as the model polyimide to investigate the plasticization phenomenon [61]. After thermal treatment at 350 °C, the 15 and 30 min heat-treated Matrimid films did not plasticize in the whole range of CO$_2$ feed pressure (up to about 40 bar, i.e., 39.48 atm). Noticeably, CO$_2$ permeability gradually approached a limiting constant value with increasing feed pressure. All thermally-treated films became insoluble. Upon pressure elevation, the 15 and 30 min heat-treated films showed up to 11% and 30% higher selectivity, respectively, compared with the untreated membranes. This can be attributed to the densification of the polymer matrix.

3.1.1. Decarboxylation-Induced Crosslinking

A novel polyimide 6FDA-DAM-DABA (2:1) has been successfully synthesized [56]. The sample quenched from above T$_g$ exhibited enhanced plasticization resistance, where plasticization pressure is about 34.02 atm (500 psi). Quenching polyimide brings a large free volume into the polyimide matrix and endows it with enhanced plasticization resistance. Through decarboxylation at high temperature (slightly below the T$_g$), thermally crosslinked polyimide linked by covalent bonds has more free volume compared to diol or diamine crosslinking agents. Thermal gravimetric analyzer (TGA) and C^{13}-NMR (nuclear magnetic resonance) measurements prove that the free acid polymer undergoes decarboxylation under such conditions. Then, the residual aryl radicals react through some generated active sites to form the crosslinked structure. Figure 4 shows possible crosslinking sites through diamines in the free acid polymer.
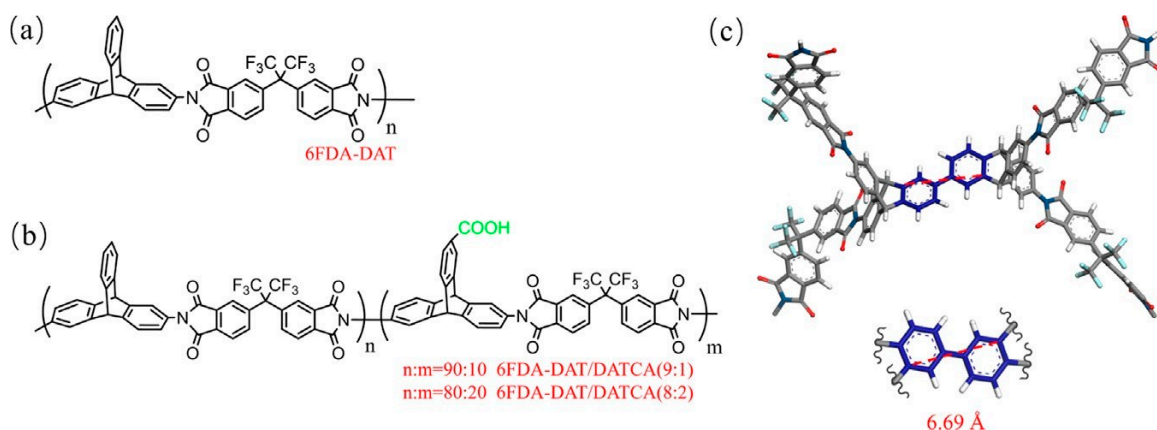
The 6FDA-DAM:DABA(3:2) polyimide was prepared by tuning the proportion of monomers in order to study the effect of thermal treatment on plasticization resistance [57]. The results revealed that thermally crosslinked membranes showed no signs of plasticization up to 47.63 atm (700 psi) for pure CO$_2$ gas, or 1000 psi for 50/50 CO$_2$/CH$_4$ mixed-gas separation.
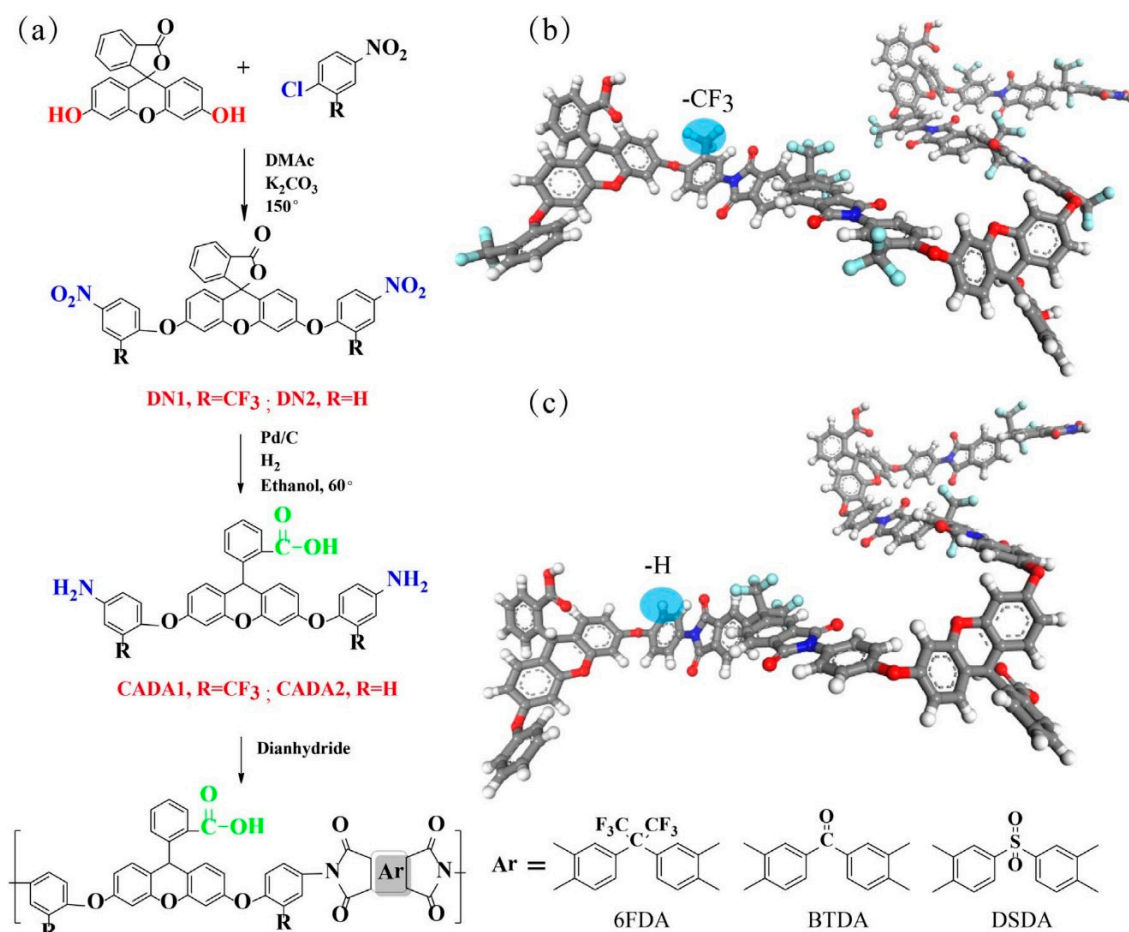
A

B

C

Figure 4. Possible crosslinking sites through diamines in the free acid polymer: (**A**) through the DAM methyl; (**B**) biphenyl crosslink; and (**C**) at the cleaved CF_3 site [56].

Triptycene—a rigid three-dimensional (3D) symmetric structure with a 120° included angle of two benzene rings—can dramatically disturb polymer chain packing and enlarge polymer free volumes. Therefore, introducing triptycene building units into polymer chains should enhance permeability performance. Three triptycene-based polymers, including 6FDA-DAT, 6FDA-DAT/DATCA (9:1), and 6FDA-DAT/DATCA (8:2), were synthesized by our group [60] (DAT, 2,6-diaminotriptycene; and DATCA, 2,6-diaminotriptycene-14-carboxylic acid). Figure 5 shows chemical structures of 6FDA-DAT and 6FDA-DAT/DATCA. No plasticization was observed for crosslinked 6FDA-DAT/DATCA (9:1) and 6FDA-DAT/DATCA (8:2) at CO_2 pressure up to 30 atm for pure gas, and a partial CO_2 pressure up to 20 atm for (CO_2:CH_4 1:1) mixed gases. In addition, 6FDA-DAT/DATCA (9:1)-450 had the highest CO_2 pure gas permeability of 305.8 Barrer with a CO_2/CH_4 ideal selectivity of 27.8, while 6FDA-DAT/DATCA (8:2)-350 had the highest CO_2/CH_4 ideal selectivity of 43.7 with a CO_2 pure gas permeability of 58.5 Barrer.

Two carboxylic acid-containing diamines, CADA1 and CADA2, were successfully synthesized to polymerize with 6FDA, BTDA, and DSDA, respectively [58]. The synthesis route is illustrated in Figure 6. The CO_2-induced plasticization phenomenon was not observed at a CO_2 pressure up to 30 atm for 6FDA-CADA1-425, which had a CO_2 permeability of 917.4 Barrer with a CO_2/CH_4 ideal selectivity of 28.11.
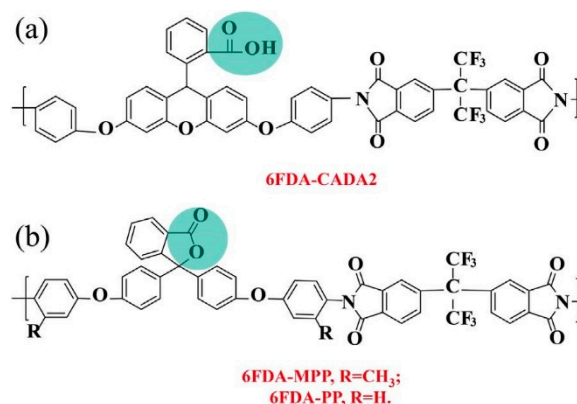
Figure 5. Chemical structures of (**a**) 6FDA-DAT; (**b**) 6FDA-DAT/DATCA; and (**c**) estimated distance (6.69 Å) between the crosslinked chain segments of 6FDA-DAT/DATCA (energy of chain conformations was minimized using Material Studio 7.0) [60].

Figure 6. (**a**) Synthesis routes of dinitro monomers, diamines as well as and 6FDA-, BTDA-, and DSDA-based carboxylic acid-containing polyimides, (**b**) and (**c**) show the energy-minimized chain conformations of 6FDA-CADA1 and 6FDA-CADA2 polymers, respectively (using Material Studio 7.0) [58].

In the above work, the temperature sufficient to complete the crosslink reaction was 425 °C, which is higher than the T_g of most polymers. Therefore, the follow-up objective was to lower the crosslinking temperature, by adopting two phenolphthalein-based polyimides, 6FDA-MPP and 6FDA-PP [59]. Figure 7 shows chemical structures of 6FDA-CADA2, 6FDA-MPP, and 6FDA-PP. No plasticization

was observed in the 6FDA-MPP-400 and 6FDA-PP-400 polyimides at a CO_2 pressure up to 30.62 atm (450 psi). The results found that 6FDA-MPP-400 obtained the best performance with a CO_2/CH_4 ideal selectivity of 39.2 and a CO_2 permeability of 193.8 Barrer.
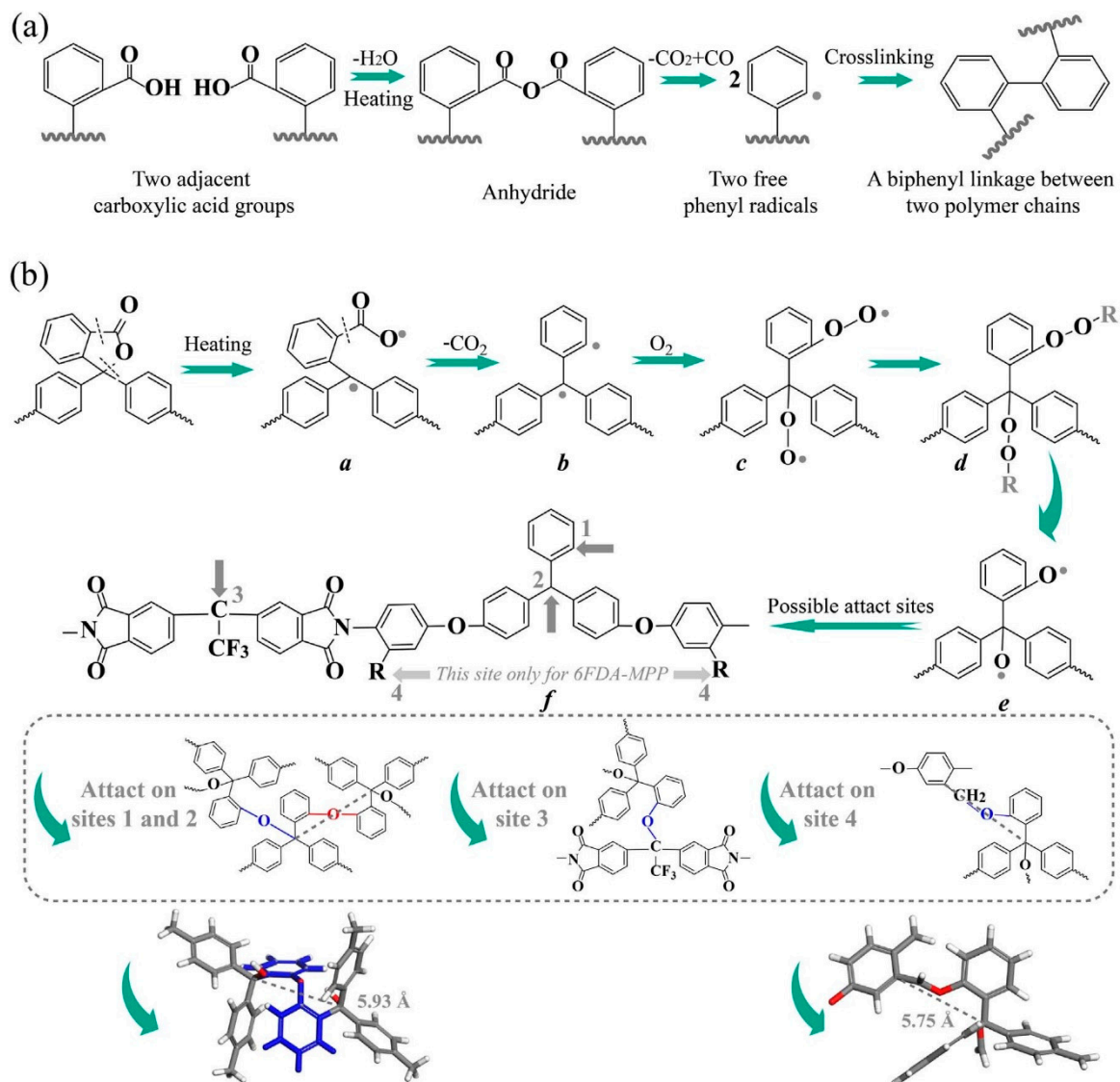

Figure 7. Chemical structures of (**a**) 6FDA-CADA2 [26], and (**b**) 6FDA-MPP, 6FDA-PP [59].

Figure 8 illustrates two different mechanisms, revealing how polymer chains crosslink under thermal treatment. The free carboxylic acid groups exist along the polymer chains, allowing the polymers to go through a series of changes (Figure 8a). Polymers containing lactone rings are supposed to cleave their lactone ring, which directly decomposes causing polymer chain breaks. Such types of crosslink reactions occur in the presence of oxygen (heated in air atmosphere). This thermal oxidative crosslinking method is widely applied during the preparation of carbon molecular sieve (CMS) membranes. In our current work, the crosslinking temperature of the lactone ring containing polyimides significantly decreased to 350 °C, which is lower than the pre-polymer's glass transition temperature. If the lactone ring-based polyimide is adopted to spin hollow fiber membranes, the porous substrate of the membrane will be preserved during thermal oxidative crosslinking.
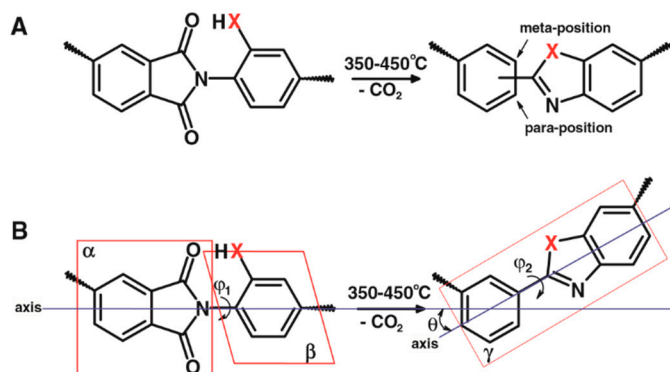
3.1.2. Thermally Rearranged (TR) Polymers

Thermally rearranged (TR) polymers are highly permeable polymers that, at high temperatures, convert polyimide or polyamide into heterocyclic polybenzothiazole (PBT) or polybenzoxazole (PBO). It was originally proposed that polyimides containing ortho-positioned functional groups (for example –OH) can be used to prepare rearranged polymers with altered chain pain packing, with confined spatial location due to the thermal rearrangement [62]. Figure 9 shows changes in conformation–polymer chains and spatial relocation due to chain rearrangement in confinement. As a result, TR polymers show excellent resistance to plasticization at CO_2 partial pressure as high as 20 atm. In contrast to glassy polymers, TR polymer membranes do not exhibit substantially reduced selectivity, even at elevated CO_2 fugacity (~15 atm).

Some TR polymers show strong resistance to plasticization. For the polyimide synthesized from 3,3'-dihydroxy-4,4'-diamino-biphenyl (HAB) and 6FDA (hexafluoroisopropylidene-diphtalic anhydride), pure CO_2 permeation curves pass through a minimum pressure at about 20 atm, which then begins to increase [63]. However, when the HAB–6FDA polyimide precursor were converted to polybenzoxazole (PBO) by heating under flowing N_2, plasticization pressure points were not observed for CO_2 up to 25 atm. In addition, more TR conversion would result in a higher permeability of CO_2 and CH_4, as well as higher plasticization fugacity than those of the polyimide.

Figure 8. (**a**) The thermal crosslinking mechanism of carboxylic acid-containing polyimides, and (**b**) the thermal oxidative crosslinking mechanism of phenolphthalein-based polyimides as well as the energy-minimized distances between the possible crosslinking sites estimated using Material Studio 7.0 [59].

Figure 9. (**A**) Changes in conformation–polymer chains consisting of meta- and/or para-linked chain conformations can be created via rearrangement. (**B**) Spatial relocation due to chain rearrangement in confinement, which may lead to the generation of free-volume elements [62].

3.2. Chemical Crosslinking

When polymer chains are chemically crosslinked by covalent bonds, the crosslink networks are quite stable in harsh environments and can sufficiently inhibit the rotation of polymer chains. Polyimides contain many activated sites on polymer chains that are able to establish covalent bonds.

Typical reactive sites are imide bonds. In theory, all polyimides can be crosslinked on their imide groups and show improved plasticization resistance. Crosslink networks can also be tailored according to the characteristic functional group of specific polymers. This method with an encouraging prospect is shown in Section 3.2.1.

Beyond using imide bonds as crosslinking sites, the crosslinking reaction can also take place through reactive functional groups and other crosslinking agents as introduced in Sections 3.2.2–3.2.4.

3.2.1. Polyamine Crosslinking

Imide bonds in polyimide membranes can react with specific diamine monomers to cleave the imide ring, thereby crosslinking the polymer chains. This is a promising approach to crosslink polyimide membranes, which possess the imide bond. Introducing amine bonds further introduces improved properties such as hydrophilicity and stability in solvents.

To collectively optimize the permeability and selectivity, the molecular structure and steric constraints must be considered as key factors. In addition, different kinds of diamines react distinctly when crosslinked with polyimide chains. Some factors that are less related to diamines themselves, may also play critical roles in the performance of polyimide membranes such as side-reactions and degree of crosslinking.

Previous work has reported on the crosslinking of monomeric and polymeric diamines with polyimide membranes. Figure 10 illustrates some diamines acting as the crosslinkers reported in the literature. Monomeric diamines fall into two classes: aliphatic and aromatic diamines.
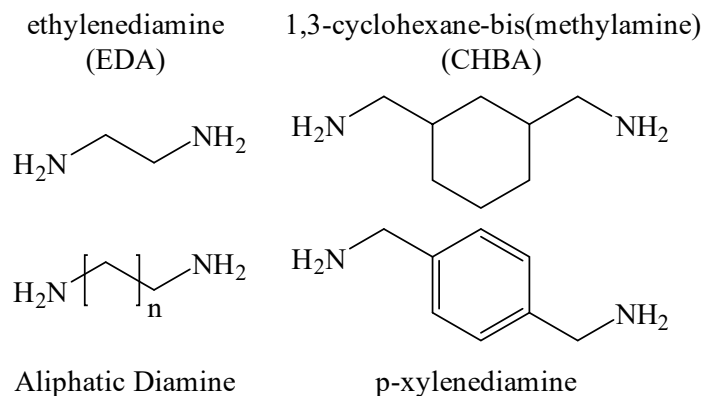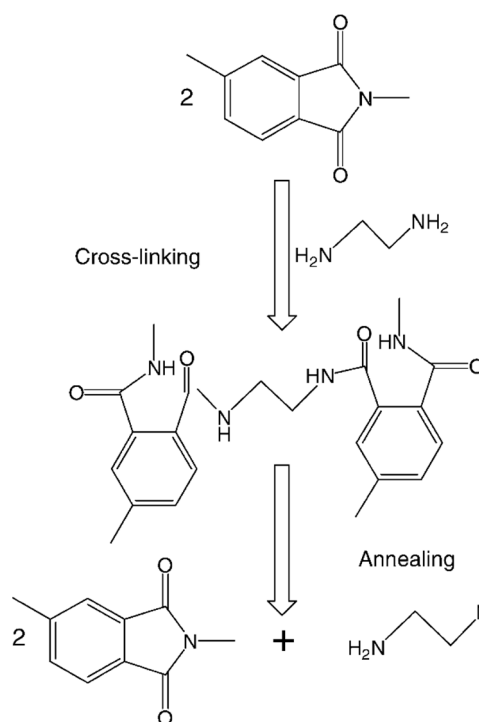

Figure 10. Diamine monomers used in the literature.

This crosslinking method is often followed by thermal treatment to enhance CO_2 plasticization resistance. However, thermal treatment may lead to the release of diamine monomers and decomposition of the crosslinked polymer networks.

Diamine-Monomer Crosslinking

Shao et al. chose 1,2-ethylene diamine (EDA)—a linear aliphatic diamine—to prepare crosslinked 6FDA-durene, and then treated the membrane material with thermal annealing at 250 °C [64]. The modified membrane material exhibited plasticization pressure at 48.99 atm (720 psi), while the original 6FDA-durene membrane was plasticized by CO_2 at 300 psi. The imide bonds reacted with EDA, resulting in imide ring cleavage. EDA monomers then connected two polymer chains through their amide bonds. The insertion of crosslinking agents into polymer chains significantly decreased the

d-space, bringing about the structure-tightening effect. Figure 11 shows possible reaction mechanisms during 1,2-ethylene diamine (EDA)-induced cross-linking and thermal annealing.

Figure 11. Possible reaction mechanisms during 1,2-ethylene diamine (EDA)-induced cross-linking and thermal annealing [64].
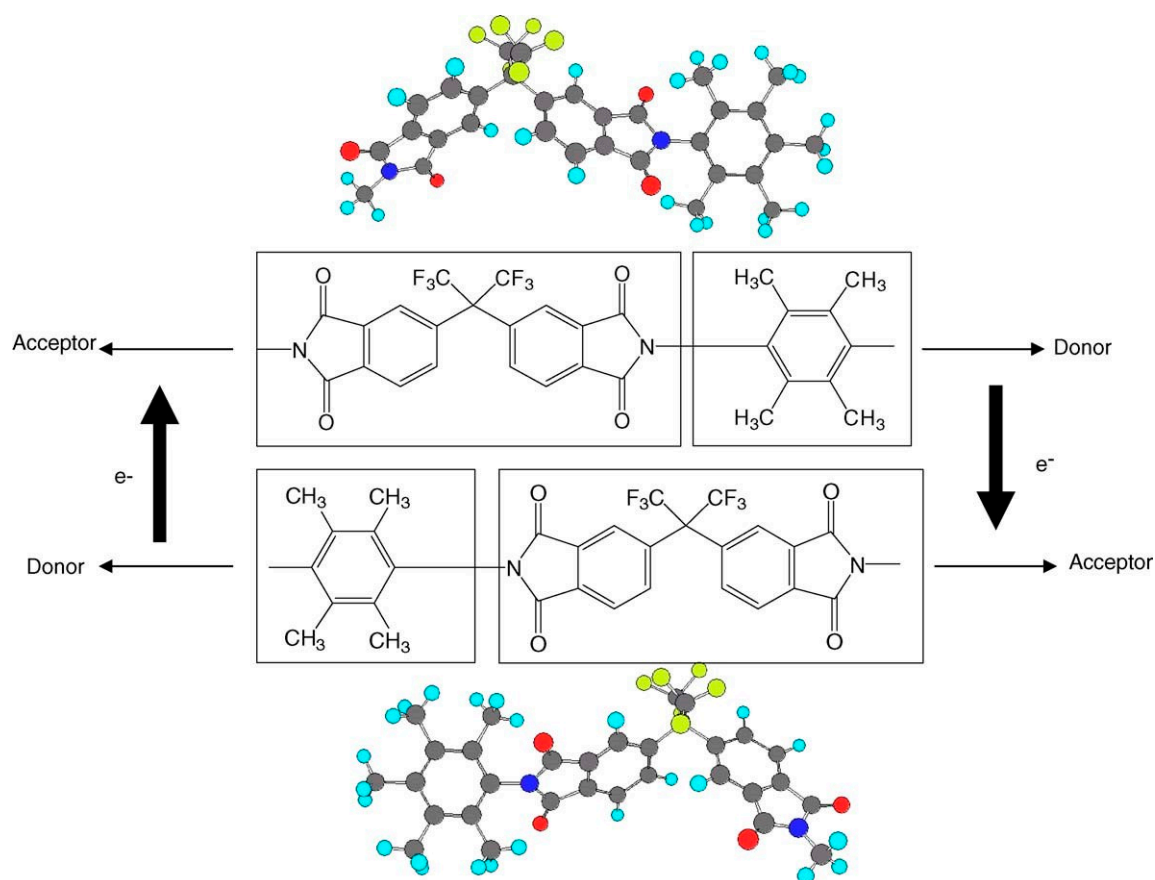
The subsequent thermal annealing triggers the imidization reaction of crosslinking networks, accompanied by EDA release at specific temperatures. Higher thermal annealing temperatures achieve stronger plasticization resistance.

At the specific high temperature stage, coupling effects of EDA crosslinking and thermal annealing accelerate the formation of charge transfer complexes (CTCs). As a consequence, polymer chain mobility decreases, the membrane matrix becomes denser, and the membranes' color changes from transparent to yellow. Shao et al. ultimately found two approaches to enhance the anti-plasticization properties: (1) A shorter EDA crosslinking time followed by a higher annealing temperature, or (2) a longer EDA crosslinking time followed by a lower annealing temperature.

It is a remarkable fact that a single treatment, polyamine crosslinking or heating, cannot strongly suppress the plasticization. Plasticization resistance will be enhanced only if the polymers are crosslinked by polyamine molecules first, followed by thermal treatment. This is proven by several experimental phenomena. The original 6FDA-durene was still transparent after heating at 250 °C in vacuum, which indicates that 250 °C thermal annealing on the original 6FDA-durene could not induce CTC formation. Compared to the original, easier membrane plasticization was achieved after 1-min EDA cross-linking. In summary, only the coupling effects of EDA cross-linking and thermal annealing may facilitate the formation of CTCs in bulk 6FDA-durene, to achieve the desired anti-plasticization effect.

6FDA-durene membranes can also be crosslinked with 1,3-cyclohexanebis (methylamine) (CHBA); the modified membranes showed no obvious plasticization up to 48.99 atm (720 psi) [65]. The reaction mechanism during the chemical crosslinking and thermal annealing is similar to membranes modified by EDA. Although the thermal treatment regenerates imide groups from amide groups in the crosslinked networks, polyimide membranes micro-structures exhibit irreversible changes. Unlike EDA-modified membranes, crosslinking in the CHBA/methanol solution facilitates the diffusion of

crosslinking agents through the membranes to react with the bulky body, because methanol swells the membranes. Thermal annealing almost homogeneously changes the chemical composition and structure of the crosslinked polyimide matrix. Therefore, in this case, membranes are not only modified on the surface, but also in the body. Diamine monomers open the main chains in the membranes' matrix, increasing polymer chain flexibility. This relative flexibility tends to achieve configurational rearrangement and forms CTCs, especially at higher temperatures (200 °C in this case). Figure 12 shows charge transfer complex model of 6FDA-durene polyimides. Thermal annealing induces the regeneration of chemical composition from amide groups to imide groups. However, the formation of CTCs restricts the mobility of polymer chains. These two factors contribute to enhancing anti-plasticization characteristics.
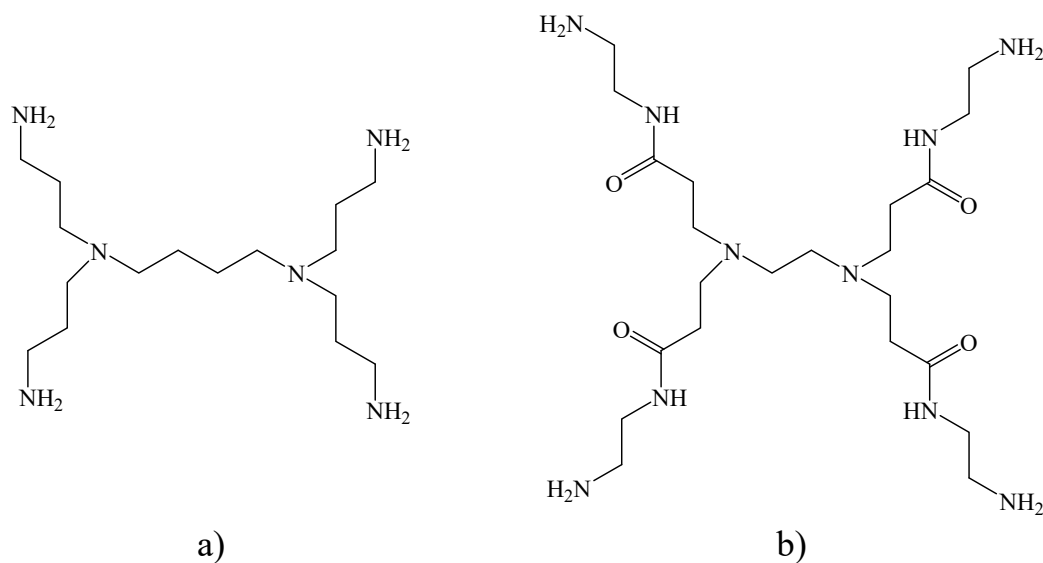

Figure 12. Charge transfer complex model of 6FDA-durene polyimides [65].

The commercially available polyimide, Matrimid, can be crosslinked with *p*-xylenediamine to restrict plasticization [67]. The permeability of 30-day crosslinked membranes remains constant in the whole range of CO_2 feed pressure (from 3.55 to 32.4 atm). The crosslink reaction can be detected by measuring the gel content. Compared with fluoropolyimides such as 6FDA-durene, Matrimid has less free volume and swelling degree in methanol [83]. Therefore, it takes the Matrimid membrane matrix longer to swell in methanol. Furthermore, membrane swelling in methanol is the rate-determining step, thus the crosslinking rate of Matrimid is much lower than those of fluoropolyimides.

Amine-Tetramer, Dendrimer Crosslinking

Diamines and tetramines—dendrimers containing four free amine groups—can be used as crosslinkers such as polyamidoamine (PAMAM) and diaminobutane (DAB). Their chemical structures are shown in Figure 13.

Figure 13. Chemical structures of (**a**) diaminobutane (DAB), and (**b**) polyamidoamine (PAMAM).

Xiao et al. combined PAMAM crosslinking with thermal treatment methods, but did not observe the plasticization phenomenon up to 30 atm [66]. The start temperature of PAMAM decomposition was previous to the thermal degradation of PAMAM-modified polyimide membranes. In addition, thermal stability decrease of the PAMAM-modified polyimide from 593 to 579 °C was unexpected. The X-ray photoelectron spectroscopy (XPS) data proved that thermal treatment of PAMAM-modified polyimide films at 250 °C brought about imidization of poly(amic amide), and the thermal decomposition of the PAMAM dendrimer. ^{1}H nuclear magnetic resonance (NMR) indicated that PAMAM dendrimers are cleaved into small molecules at 250 °C. When heating membrane materials, PAMAM presence in polyimide degrades polyimide chains to low molecular weight fragments with lower thermal stability. Heat treatment increases inter-segmental mobility, thus increasing the likelihood of PAMAM dendrimer free primary amine groups meeting the imide groups in the polyimide backbone. However, high temperature treatments induce significant dendrimer decomposition at the amide linkage, leading to crosslinked structure breakdown. They also result in the degradation of polyimide, which may produce a heterodispersed population of compounds with lower molecular weights. A high temperature treatment induces a higher degree of crosslinking, which tightens the polymer chains and limits intersegmental chain mobility. Therefore, thermal treatments at 120 °C offer better plasticization resistance than simple immersion modifications. Interestingly, modified films treated at 250 °C exhibited stronger plasticization compared with the original polyimide films. The most likely explanation is that the 250 °C treatment rebuilds the imide ring in the main polymer backbone, and enhances chain rigidity. At the same time, CTCs formation between neighboring polyimide chains helps decrease CO_2 sorption, reduce chain mobility, and stabilizes the structure.

Although many polyamine-crosslinked polyimide membranes have been successfully synthesized, the plasticization response has not been reported, indicating a need for further research in this area. Interestingly, investigating the effect of crosslinking reagents on different polyimides has been made [84].

Immersing the membrane in a dendrimer-methanol solution can induce polymer chains crosslink. Chung et al. used PAMAM to crosslink 6FDA-durene membranes [85]. Compared with diamines, with two functional end groups, the bulk teramines exert a space-filling effect on the polymer chains to reduce d-spacing, which leads to free volume decrease. Furthermore, due to the steric hindrance of the large dendrimer molecules, it takes more time for them to diffuse into the polymer matrix. This may result in asymmetric crosslinking throughout the bulky membrane matrix. In addition, the large molecular size makes the decreasing rate of the diffusion coefficients of PAMAM crosslinked polymers significantly slower than using other crosslinking agents containing amino groups. The initial increase

in gas solubility with immersion time may be attributed to two factors: one is that PAMAM contains all kinds of amine groups such as –NH$_2$, –NH–, or –N<. These amines groups have strong interactions with CO$_2$, resulting in the increase of CO$_2$ solubility of polyimides; the other possible reason is that the big molecular size of dendrimers may slightly increase the interstitial space, which may result in greater adsorption. However, the plasticization response was not reported in this work.

The effect of modification time and the generations of the PAMAM dendrimer on the properties of modified polyimide films has been reported [86]. When it is only dried at room temperature, some free primary amine groups for the loaded PAMAM dendrimers remain on the surface of polyimide films.

DAB dendrimers, a crosslinking agent for polyimides, can perform crosslinking reactions at room temperature and improve gas separation performance of polyimide membranes, especially for H$_2$/N$_2$, He/N$_2$, H$_2$/CO$_2$ [87].

Polyamine Crosslinking

Compared with monomer polyamines, there have been fewer investigations on crosslinking polyimide membranes by polymeric polyamine. For instance, poly(propylene glycol) block poly(ethylene glycol) block poly(propylene glycol) diamine (PPG/PEG/PPGDA) was successfully employed to chemically crosslink Matrimid 5218 at room temperature [88].

Brief Summary

Based on the above discussion, some insights can be given into polyamine crosslinking. Only the integration of thermal annealing with polyamine crosslinking can significantly improve plasticization resistance. As polyamine crosslinking reduces the interchain spacing, the polymer chains become closer to each other. Thermal annealing enhances chain mobility, so more CTCs will be formed between the polymer chains. In conclusion, the essence of this method is to facilitate the CTCs' formation.
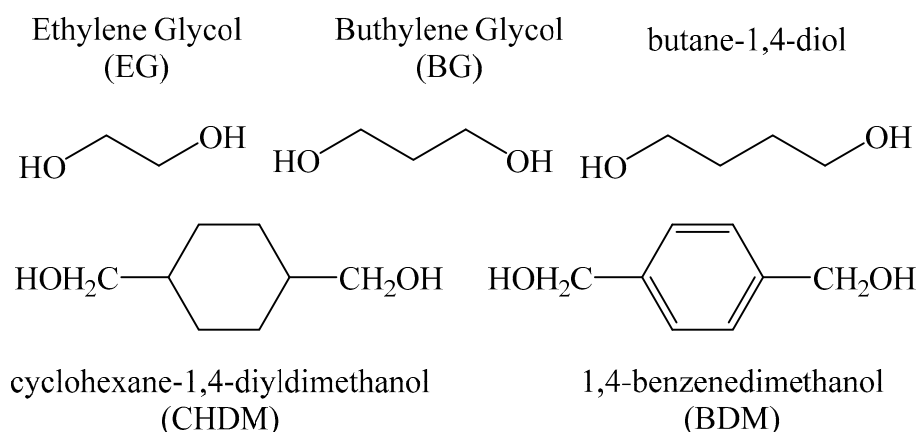
Finding a suitable polyamine and probing proper reaction protocols will be the future trend in polyamine crosslinking aimed improving plasticization resistance. Therefore, the molecular size, number of free primary amine groups, molecular rigidity and polarization, etc. must be taken into consideration.

To illustrate, consider the molecular size first: If the polyamine molecule is too small, it will decrease the d-space of the polymer chains, generating the decline of permeability; conversely, it takes a large polyamine molecule more time to achieve the desired crosslinking effect because its larger molecular size makes it harder to penetrate into the polyimide matrix. Therefore, a polyamine with a moderate molecular size is assumed to space apart the chains while stabilizing the membranes. They should be able to penetrate deeper into the polymer matrix and thus construct a thicker crosslinking layer on the surface of polyimide films.

3.2.2. Diol Crosslinking of Carboxylated and Sulfonated Polyimide Membranes

If the polyimides have carboxylate or sulfonate groups, they can be crosslinked by diols or polyols through esterification. Unlike amine crosslinking, some diols or polyols can suppress the plasticization, while maintaining good permeability and selectivity of the original polymers. Common diol crosslinkers are shown in Figure 14.

Similar to crosslinking by polyamines, crosslinking by diols is sometimes followed by thermal treatment. Furthermore, hydrogen bond formation cannot be negligible due to the presence of carboxyl groups along the polymer backbones. The contribution made by hydrogen bonding to plasticization suppression will be discussed in Section 3.3.

Ethylene Glycol　　　　Buthylene Glycol　　　　butane-1,4-diol
(EG)　　　　　　　　　(BG)

cyclohexane-1,4-diyldimethanol　　　　　　1,4-benzenedimethanol
(CHDM)　　　　　　　　　　　　　　　　(BDM)

Figure 14. Common diol crosslinkers.

Diol Crosslinking through Carboxylic Acid Groups

Staudt-Bickel C et al. introduced –COOH groups to the polyimide backbones and crosslinked the polymer with ethylene glycol [19]. The highlight of this crosslinked polymer with exquisite structure was the little plasticization up to 35 atm pure CO_2 pressure accompanied by increased CO_2/CH_4 selectivity. The strong crosslinked 6FDA-DABA exhibited much better CO_2/CH_4 separation properties with an ideal selectivity of 87 and a CO_2 permeability of 10.4 Barrer at 3.74 atm and 308 K. 6FDA-6FpDA/DABA crosslinked with ethylene glycol (EG) can stabilize the membrane much more effectively, leading to plasticization pressure increase [41].

The cyclohexane-1,4-diyldimethanol (CHDM) monoester can also be used in esterification crosslinking. The plasticization pressure correlated with a sorbed CO_2 partial molar volume of 29 ± 2 cm^3/mol in the polymer [68]. However, the exact plasticization pressure was not reported.

To find the initial principle of choosing a diol crosslinker, the effects of length and flexibility of various diol crosslinking agents has been investigated [69]. In view of high permeability with reasonable CO_2/CH_4 selectivity, 6FDA-DAM:DABA 2:1 was used as a model polymer. The esterification reaction was shown to be effective in stabilizing membranes against CO_2 plasticization up to 40 atm feed pressure. Compared with untreated 6FDA-DAM:DABA membranes, the incorporation of DABA increased selectivity. 6FDA-DAM:DABA crosslinked with buthylene glycol (BG) obtained the highest selectivity of 34 among the crosslinked samples.

6FDA-DAM:DABA and 6FDA-6FpDA:DABA copolymers have been synthesized for crosslinking with BG and CHDM [89]. CO_2 permeabilities increased by factors of 4.1 and 2.4, respectively, at 20 atm feed pressure, without loss in selectivity. Furthermore, selectivity increased with higher crosslinking density for feed pressure below 20 atm. The 6FDA-DAM:DABA 2:1 membranes crosslinked with CHDM showed a CO_2/CH_4 selectivity of 32-33, while the membranes crosslinked with BG exhibited similar selectivity performance with a CO_2/CH_4 selectivity of 33.

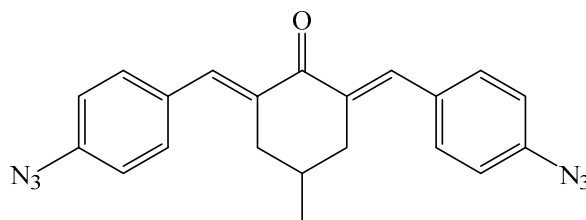Diol Crosslinking through Sulfonic Acid Groups

Sulfonic acid groups along the polymer chains can react with diol molecules to form ester bonds linking the two polymer chains. The reaction mechanism of the sulfonic acid group resembles the mechanism of the carboxylic acid group discussed above. Although this crosslinking method has been successfully applied in various separation processes [90,91], no report has been found in the field of polyimide membranes in gas separation applications.

3.2.3. Semi-Interpenetrating Network

The construction of crosslink networks can be obtained from multiple types of polymer chains, and by crosslinking polymer chains with another polymer network. Some reactive monomers containing functional groups can chemically crosslink or physically interlock the linear polyimide

chains, while solely reacting with its species to form a polymer network. The introduction of these reactive monomers can tune the size and quantity of the cavities. Furthermore, the free volume distribution of the pseudo-interpenetrating networks (pseudo-IPNs) may be beneficial for the separation of small molecules by polymeric membranes, due to both the mean cavity size and the quantity of free volume influencing polymeric membranes permeability.

In situ polymerization of azido monomers tends to form oligomer networks. Simultaneously, functional groups within the network react with specific sites on polymer chains to form semi-interpenetrating networks, resulting in a membrane with no signs of plasticization up to 30 atm [72]. The chemical structure of the azide used in this paper is shown in Figure 15. Azide introduces the azido group, a linear 1,3-dipolar structure, into the membrane matrix. Upon heating or under ultraviolet radiation, azido groups are able to create nitrene—a highly reactive, short-lived intermediate. Nitrenes insert into C–H bonds and add to unsaturated C–C bonds such as alkenes, alkynes, and arenes due to their electrophilicity. These data indicate that every kind of polyimide has the potential to react with azide. In general, the reactive priority of the C–H insertion follows this sequence: tertiary > secondary > primary C–H bonds. Functional groups cable of reacting with nitrene are: (1) Phenyl groups of azide or host polyimide; (2) –CH_3 substituent groups of azide or host polyimide; (3) the –CH_2– group in the cyclohexanone structure of azide; and (4) α,β-unsaturated ketone of azide. First, C–H bonds of phenyl groups are not easily attacked by nitrene radicals, owing to the benzene ring stability, which comprises the highly conjugated π electrons. Although the unfavorable addition of nitrene to C=C bonds has been reported, the absence of the characteristic peak of tertiary amine indicates that the cycloaddition of nitrenes to the phenyl ring and the C=C bonds has not occurred. Second, due to steric hindrance, there is no reaction with alkenes. Azide can, therefore, react with its own species to form polymer networks, and with the functional groups of the host polyimide to form an interconnected pseudo-IPN. Therefore, for those polyimide membranes containing no functional groups to react with nitrenes, such as 6FDA-NDA, the combination of polyimide and poly(azide) only results in a pseudo-IPN without any interconnection (NDA is short for "1,5-naphthalenediamine").
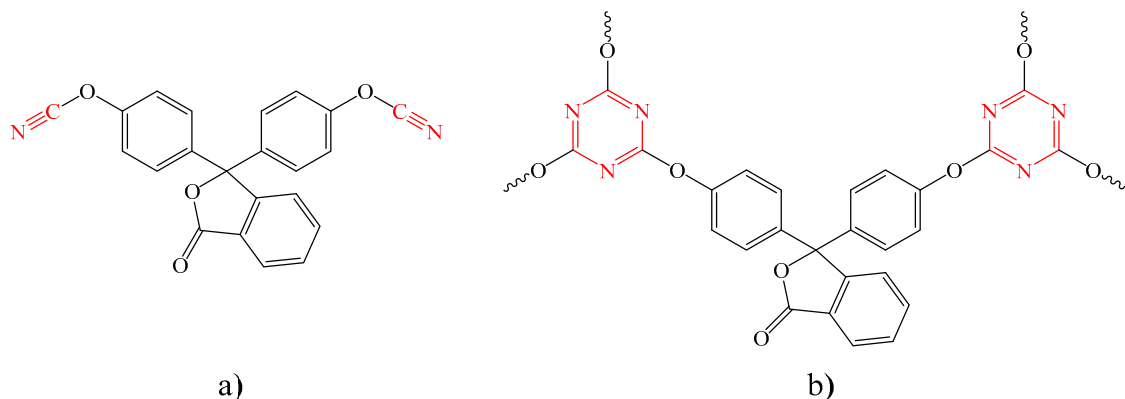

Figure 15. Chemical structure of 2,6-bis(4-azidobenzylidene)-4-methylcyclohexanone.

As the insoluble gel in the film reflects the formation of crosslinked networks, it can be inferred that nitrene radicals react with the methyl C–H bonds of 6FDA-TMPDA to form chemical crosslinks (TMPDA is short for "2,3,5,6-tetramethyl-1,4-phenylenediamine"). The formation of denser interconnected pseudo-IPNs restricts chain movement and enhances the anti-plasticization property of the material.
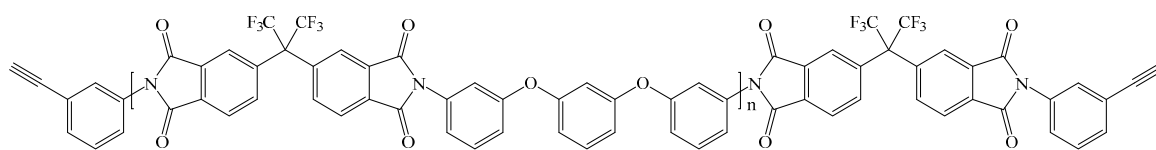
Another crosslinker, phenolphthalein dicyanate (DCFT), has been shown to improve plasticization resistance. Chemical structures of DCFT and DCFT-resin are shown in Figure 16. DCFT-modified membranes did not show any signs of plasticization in CO_2 feed pressures ranging from 1 to 30 atm [71]. Dicyanate cyclotrimerized into a uniform three-dimensional network of oxygen-linked triazine rings (cyanurate ester resin). The absence of by-products was indicated by the ^{1}H NMR, elemental analysis, and mass spectrometry data. It is worth noting that copper naphthenate and nonylphenol serving as a catalyst must be added to mitigate curing temperatures from 280 °C to 180 °C. The results of Fourier transform infrared spectroscopy (FTIR) and differential scanning calorimetry (DSC) showed that after heat treatment at 180 °C for 60 min, dicyanate seemed to be entirely converted into the corresponding

cyanurate ester resin. DCFT introduces cyanurate ester resin into the Matrimid matrix, which causes a compacting effect. Hence, all semi-IPNs showed a higher density compared to Matrimid films, indicating the densification of semi-IPNs. Consequently, this densification effect successfully restricts plasticization by hindering polymer chain mobility.

Figure 16. Chemical structures of (**a**) phenolphthalein dicyanate (DCFT), and (**b**) cyanurate ester resin (DCFT-Resin).

Except for highly reactive monomers, oligomer-containing functional groups can also be used to form semi-IPNs together with host polyimides. It is well-known that the use of longer oligomer chains results in improved toughness. Bos et al. used Thermid FA-700 as a crosslinker to resist plasticization effectively [36]. Figure 17 illustrates chemical structure of Thermid FA-700. Modified films showed a constant permeability at elevated pressure in the pressure range (up to 50 bar, i.e., 49.35 atm) of the CO_2 permeability test. It has been already proven that the acetylenic end group can be crosslinked by heating at 250–275 °C without the evolution of volatile products, while the oligomer polymerizes [92]. Two kinds of crosslinking reactions are likely to happen: (1) the benzenoid cyclization (crosslinking) reaction, i.e., trimerization reaction of the acetylene groups; and (2) the naphthalene formation (polymerization) reaction. These reactions form semi-IPNs. Compared with the Matrimid/Thermid film without heat treatment, thermal annealing triggers a crosslinking reaction between the oligomer and Matrimid, which leads to the obvious suppression of plasticization.

Figure 17. Chemical structure of Thermid FA-700.

3.2.4. Ionic Bonding

Apart from inserting covalent bonds into polymer chains, an alternative strategy entails connecting polymer chains with ionic bonds. A prerequisite for the formation of ionic bonds is the presence of an electron donor or acceptor along the polymer backbone, which can be carried out by the substitution reaction.

It has been reported that the introduction of bromine into polymer constitutional units by bromination of 6FDA-durene, allows crosslinking of the original membrane to N,N′-dimethylpiperazine [73]. This electrostatic chemical bond effectively restricts polymer chain mobility and somewhat stabilizes the CO_2/N_2 selectivity. As a result, membranes did not show an upturn of permeability in the isotherm within the experimental scale of 25 atm of CO_2. It is remarkable that the pendant piperazinium-mediated crosslinked polyimide membranes displayed a high CO_2
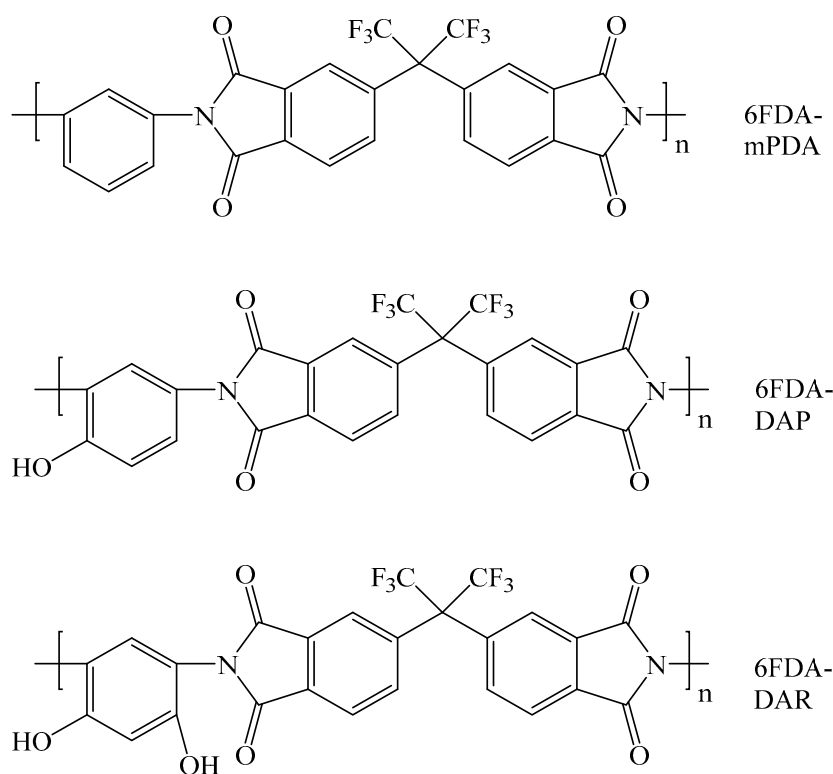
permeability of 475.5 Barrer, together with high CO_2/CH_4 and CO_2/N_2 permselectivities of 34.5 and 18, respectively.

3.3. Physical Crosslinking

The introduction of polar functional groups, such as hydroxyl and carboxyl groups, that can form hydrogen bonds, leads to CTCs and pseudo-crosslink networks formation. To present a larger picture of the physical crosslinking method, mixed matrix membranes are also discussed in this section.

3.3.1. Hydroxyl Group

Alaslai et al. prepared three polyimides with different numbers of hydroxyl groups (shown in Figure 18), and demonstrated that polyimides with strong polar –OH groups could mitigate plasticization when tested under high-pressure binary CO_2/CH_4 mixed-gas conditions due to strong chain interactions by inter-chain hydrogen bonding and CTC formation [93]. Compared with 6FDA-mPDA, hydroxyl-containing polyimide membranes maintained very high CO_2/CH_4 selectivity (~75 at CO_2 partial pressure of 10 atm) due to high CO_2 plasticization resistance when tested under high-pressure mixed-gas conditions.

Figure 18. Chemical structures of 6FDA-mPDA, 6FDA-DAP, and 6FDA-DAR.

3.3.2. Carboxyl Group

It is well-known that the majority of carboxylic acids often exist as dimeric pairs in non-polar media. Structure of associated carboxylic acids is depicted in Figure 19. These strong polar-associating functional groups, without the formation of any covalent bonds, participate in a reversible process and are subject to media polarity and system temperature.
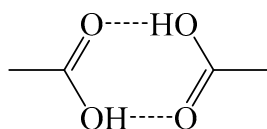
Figure 19. Structure of associated carboxylic acids.

Staudt-Bickel et al. found that polymer chains of polyimides were crosslinked by hydrogen bonding between the free carboxylic acid groups, which resulted in a strong reduction in permeability [19]. The effect of such "virtual" hydrogen bonded crosslinks on plasticization has not been reported. Additionally, an increased CO_2/CH_4 selectivity corresponds to an increased degree of crosslinking, attributed to reduced swelling and polymer chain mobility. Even with a 10% degree of crosslinking, a 20% increased selectivity can be seen in comparison to the reference polyimide. However, hydrogen bonding accounting for the formation of CTCs in the blends does well to inhibit plasticization. This will be elaborated in Section 3.5.

3.3.3. Mixed Matrix Membranes (MMMs)

Polymer membranes suffer not only from plasticization, but also permeability–selectivity trade-off limitations. These undesired phenomena can be eliminated by preparing mixed matrix membranes [94]. MMMs reported in the literature can be classified as: solid/polymer; liquid/polymer, and solid/liquid–polymer MMMs [95]. For solid/polymer MMMs, the integration of organic and/or inorganic fillers such as carbon nanotubes, carbon molecular sieves [96,97], activated carbon [98–100], zeolites [101,102], silica [103–105], and metal organic frameworks (MOFs) [106–108] can improve plasticization resistance.

Zeolitic imidazolate frameworks (ZIFs) are a sub-class of metal organic frameworks (MOFs). ZIFs show superior thermal and chemical stability, and are inherently more compatible with polymer matrix [109]. Some studies have found that the introduction of ZIF-8 (Zn (2-methylimidazole)$_2$) can improve the anti-plasticization performance of pure polymer membranes [74,75].

6FDA-durene/DABA co-polyimides were selected as polymer matrix due to their impressive performance during CO_2/CH_4 and C_3H_6/C_3H_8 separation [74]. MMMs synthesized from cross-linkable co-polyimides (6FDA-Durene/DABA (9/1) and 6FDA-Durene/DABA (7/3)), showed significant enhancements in plasticization suppression characteristics up to a CO_2 pressure of 30 atm after annealing at 400 °C due to the cross-linking reaction of the carboxyl in the DABA moiety. After being thermally annealed at 400 °C, the MMM made of 6FDA-Durene/DABA (9/1) with 20 wt% ZIF-8, showed a CO_2/CH_4 selectivity of 19.61 and an impressive CO_2 permeability 728 Barrer in the mixed gas tests.

Instead of a sharp ZIF-8 crystal, blending 10 wt% blunt ZIF-8 in the waste polystyrene (*w*-PS) container-derived membrane matrix showed good aging resistance and improved anti-plasticization gas separation performance [75]. CO_2 permeability of pure PS membranes increased as CO_2 pressure increased to 3 bar (i.e., 2.96 atm). In contrast, MMMs displayed slightly increased permeability at increased operating pressure.
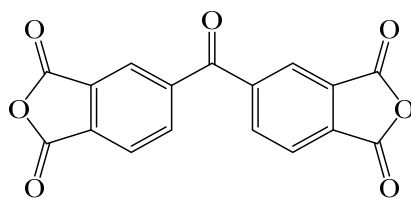
Except for ZIF-8, zeolite T was used as a filler embedded in the membrane matrix. A quantity of 1 wt% loaded zeolite T/6FDA-durene MMM showed improvement at a CO_2 plasticization pressure to 20 bar (i.e., 19.74 atm) when compared to the pristine 6FDA-durene membrane, which was plasticized at a CO_2 pressure of 5 bar [76]. CO_2 permeability and CO_2/CH_4 ideal selectivity of the MMM also increased to 843.6 Barrer and 19.1, respectively.

Investigations show that the addition of three distinctively different MOFs (MIL-53(Al) (breathing MOF), ZIF-8 (flexible MOF), and Cu_3BTC_2 (rigid MOF)) dispersed in a Matrimid polyimide can somewhat alleviate plasticization [77]. At pressures higher than the plasticization pressure of neat Matrimid (10–12 bar), the permeabilities of all MOF–MMMs slightly increased when compared with the native polymer. Additionally, the plasticization pressure increased with the MOF loading.

Incorporating Ni$_2$(dobdc) (dobdc^{4-} = dioxidobenzenedicarboxylate) metal organic framework nanocrystals into various polyimides (Matrimid, 6FDA-DAT:DAM (1:1), and 6FDA-DAM) improves the performance of their anti-plasticization properties [78]. Compared with the pristine polyimides, plasticized at around 10–15 bar, Ni$_2$(dobdc)/polyimide composites showed no sign of plasticization at a CO$_2$ partial pressure <30 bar. The separation performance of composite membranes was closer to the Robeson upper bound of the CO$_2$/CH$_4$ gas pair when compared with the pristine polymer, especially at high CO$_2$ pressure, thus indicating better anti-plasticization properties. These, along with the solution processability of the mixed-matrix format, make Ni$_2$(dobdc)/polyimides intriguing materials for commercial membrane applications.
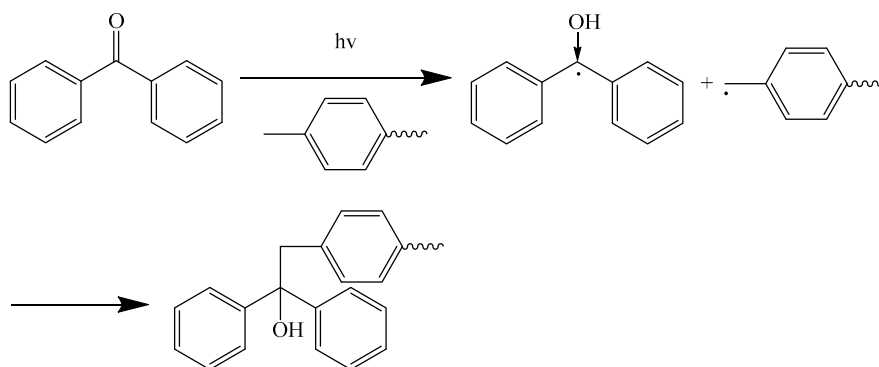
3.4. Ultraviolet (UV) Radiation Crosslinking

UV radiation is a post-treatment, which is used after membrane fabrication [110,111]. When the main chain of polyimide contains a specific structure like benzophenone, it can be crosslinked by UV radiation. Take 3,3′,4,4′-benzophenonetetracarboxylicdianhydride (BTDA) for example, the carbonyl bridge of the dianhydride is a photoactive group and serves as a UV crosslinking site. Figure 20 shows chemical structure of BTDA. The reaction mechanism of UV crosslinking of BTDA is shown in Figure 21. Radiation time, intensity, and the distance between the membrane and light source will all affect the degree of crosslinking. Thus, the degree of crosslinking of these UV-crosslinked membrane materials strongly depends on the experimental conditions.

3,3',4,4'-Benzophenonetetracarboxylicdianhydride (BTDA)

Figure 20. Chemical structure of 3,3′,4,4′-Benzophenonetetracarboxylicdianhydride (BTDA).

Figure 21. The reaction mechanism of UV crosslinking-modified polyimide containing BTDA.

Hays et al. prepared a series of semi-flexible aromatic polyimides by polycondensation of dianhydrides with phenylene diamines having alkyl substituents on all ortho positions to the amine functions incorporating at least in part 3,3′,4,4′-benzophenone tetracarboxylic dianhydride [112]. The photochemical crosslinked polyimides membranes reveal high permeation to gases while still being able to effectively separate several combinations of gases. For instance, the oxygen permeability of this kind of polyimide does not decline too much, while the selectivity of O$_2$/N$_2$ significantly increased.

In contrast to the findings of Hays et al., Kita et al. observed that the permeability coefficients decreased with increasing UV irradiation time as a result of crosslinking [113]. This decrease can be explained by the change in diffusivity, while solubility is not greatly affected. In addition, the largest

change in selectivity was obtained for the H_2/CH_4 gas pair, which had a large difference in the molecular sizes of the constituents. It is worth noticing that the selectivity for the H_2/CH_4 separation increased by a factor of 50 after 30 min of UV irradiation with a decrease in the H_2 permeability by a factor of 5.

Liu et al. investigated a series of UV irradiation modified copolyimides prepared from 2,4,6-trimethyl-1,3-phenylenediamines (3MPDA), BTDA, and pyromellitic dianhydride (PMDA) [114]. Photochemically crosslinking modification resulted in the increasing of gas selectivity of most gas pairs and declination of gas permeability. However, for the H_2/N_2 gas pair, the crosslinked copolymer exhibited a higher H_2 permeability and H_2/N_2 selectivity.

Liu et al. also synthesized another polyimide prepared from BTDA and 2,3,5,6-tetramethyl-1,4-diphenylenediamine (4MPDA), and compared two crosslinking modification methods: putting the polyimide in an ambient environment for four months, and under UV irradiation for two or eight hours [115]. The results found that the crosslinking reaction by UV irradiation only occurred in the surface layer, but crosslinking at an ambient environment for a long time took place in the whole film. This led to a much higher crosslinking density on the membrane surface and higher gas selectivity. Therefore, the resulting crosslinked polymer had an asymmetric structure.

Although plenty of meaningful and interesting work has been done in the UV radiation crosslinking of polyimide, few researchers have focused on the anti-plasticization performance after UV radiation crosslinking. Therefore, the effect of UV crosslinking on plasticization resistance needs further investigation.

3.5. Blending

Given the obvious drawbacks of low permeability and plasticization resistance, it is natural to conceive the idea of blending polyimides with other polymers exhibiting high permeability and anti-plasticization to overcome the corresponding disadvantages.
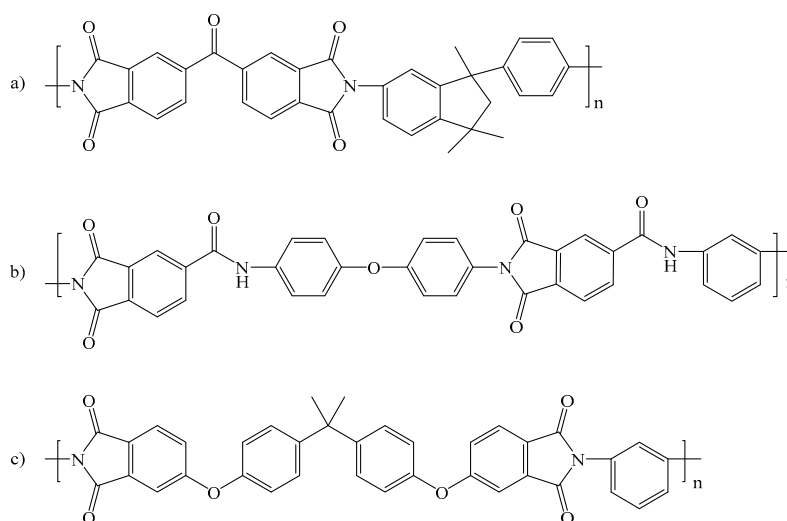
Through blending, materials may show new characteristics different from the pristine materials. Blending easily plasticized membrane materials with anti-plasticized membrane materials may improve plasticization resistance. Furthermore, blending one relatively cheaper polymer component with another more expensive component can cut down on the capital cost. Based on the above advantages, blending can be used to tailor the performance of the original single polyimide membranes.

However, not all polymers can be blended homogeneously on a molecular level. The miscibility is the most challenging problem when blending different polymers. Some coexistence modes of different polymers are well-established. For instance, one polymer may act as a dispersed or co-continuous phase in another bulky polymer matrix. Another possibility is that a single polymer may exist as an individual block mass due to the heterogeneous dispersion.

In order to prepare a blend material with superior properties, many well-designed experiments have been conducted. Polyimides, such as Matrimid, Torlon, Ultem, etc. have the ability to be blended homogeneously with a small loading of other polymers. The chemical structure of polyimides showing miscibility are depicted in Figure 22. Homogeneous blend membranes are often transparent, exhibit a single glass transition temperature, and present a clear and single phase in the polarized light microscopy (PLM) image.

To begin with, Matrimid, a commercially available polyimide, is often used in blends with other polymers to modify its low permeability. Matrimid/PSF (20/80 wt%) shows plasticization pressures up to above 30 atm [79]. The blends have been characterized by optical, morphological, and thermodynamic measurements to test the compatibility of two candidate polymer materials. No phase separation was observed with optical microscopy. DSC scans of PSF/PI blends with different compositions indicated one single glass transition temperature. It is already known that frequency shifts of miscible blends often indicate specific interactions between the characteristic groups of pure polymers. FTIR spectra shifts and intensity changes suggest PSF and PI interactions, and mixing at the molecular level. These results show that PSF and PI blending is complete and homogeneous.

Furthermore, the phase state of PSF/PI blends has been studied further by differential scanning calorimetry, rheology, and x-ray scattering [116].

Figure 22. Chemical structures of polyimides: (**a**) Matirmid® 5218, (**b**) Torlon, and (**c**) Ultem.

Bos et al. blended PSF and P84 (copolyimide of 3,3′,4,4′-benzophenone tetracarboxylic dianhydride and 80% methylphenylene-diamine + 20% methylene diamine) with Matrimid, respectively [80]. The proven homogenous blends, Matrimid/PSF (50/50 wt%) and Matrimid/P84 (60/40 wt%) were cast to form transparent membranes. Matrimid showed relatively high permeability when compared with P84, and P84 did not display an apparent signal of plasticization up to 30 atm, much higher than the critical plasticization pressure for Matrimid. Therefore, the latter blend showed a plasticization pressure of 14.80 atm (15 bar). The incomplete suppression of CO_2-plasticization at room temperature was attributed to the concentration of P84 in the blend. Moreover, the CO_2/CH_4 mixed-gas experiment of the two blends revealed a strong resistance to plasticization. The two blends showed no signs of CO_2-induced plasticization with the increasing partial CO_2 pressure in the mix gas separation test. CH_4 permeability showed a slight increase, indicating a small tendency to plasticize.

Matrimid can also be blended with carboxylated polymers of intrinsic microporosity (cPIM-1) at the molecular level [81]. The addition of cPIM-1 in Matrimid significantly enhanced the plasticization pressure for all blended membranes. A small loading of 5–10 wt% of cPIM-1 in Matrimid improved the plasticization pressure from less than 10 atm to 15 atm, while a higher loading of cPIM-1 shifted the plasticization pressure to 20 atm. The interstitial space measured by X-ray diffraction (XRD) indicated an interaction among the polymer chains between cPIM-1 and Matrimid with a reduction in interstitial space, and an enhancement in chain packing. The presence of hydrogen bonding promoted compatibility between these two polymers. The newly formed hydrogen bonds between cPIM-1 and Matrimid, integrated with the rigid polymer backbone of cPIM-1 to suppress the plasticization.

Except for Matrimid, Torlon, a rigid polyimide with superior gas-pair selectivity and intrinsic superior anti-plasticization property, can be blended with PIM-1 showing outstanding gas permeability [82]. The Torlon/cPIM-1 blends displayed plasticization pressures up to 30 atm, when compared with the pristine cPIM-1 membrane, it exhibited a plasticization pressure at around 20 atm. Hydrogen bonding between Torlon and cPIM-1 promotes polymer chain packing and reduces the fractional free volume (FFV), which accounts for this enhancement of anti-plasticization performance. The introduction of Torlon formed partial miscible blends with cPIM-1, and reduced the inter-segment mobility in the polymer matrix. It is noteworthy that cPIM-1/Torlon blend membranes, with a small amount of cPIM-1 or Torlon (5–10 wt%), can hold a homogeneous morphology. The principle of polymer blend miscibility can be testified by PLM, FTIR, DSC, TGA analyses and UV absorbance tests. A homogenous blend may present a clear and single phase in PLM images. C=O band shifts of cPIM-1

from 1700 cm^{-1} to a lower band, with an increase in Torlon loading, indicates hydrogen bonding interactions between cPIM-1 and Torlon. Moreover, the CTCs formation between cPIM-1/Torlon is demonstrated by the fact that the wavelength of the UV absorbance band of cPIM-1/Torlon blends exceeds the predicted data. The strong hydrogen bonding couples with CTC interactions to promote better compatibility between the two polymers.

Although Ultem/PIM-1 polymer blends have been reported, the plasticization resistance has not been investigated yet [117].

4. Conclusions and Prospects

In the present literature, various ways have been thoroughly discussed to restrain the typical CO_2-induced plasticization of polyimide membranes, which contribute to providing a big picture of the research findings in this field. To improve the currently existing methods and develop novel methods, the mechanisms and processes of plasticization were explored.

Taken together, there are rarely any common methods that can be applied to the majority of polyimide membranes to suppress plasticization. The most effective ways vary from membrane to membrane. Therefore, researchers should conceive of specific methods according to the specific chemical molecular structure.

Many novel and effective crosslinking methods for polyimide membranes, such as hyperbranched polyimides have yielded good performance in gas separation. Nevertheless, the plasticization response has not been reported. Therefore, this unexploited area may be one of the directions that will contribute to synthesizing the next potential polyimide membranes with good plasticization resistance.

References

1. Dung, E.J.; Bombom, L.S.; Agusomu, T.D. The effects of gas flaring on crops in the niger delta, nigeria. *GeoJournal* **2008**, *73*, 297–305. [CrossRef]
2. Kidnay, A.; Kidnay, A.; Parrish, W.; McCartney, D. *Fundamentals of Natural Gas Processing*, 2nd ed.; CRC Press: Boca Raton, FL, USA, 2011.
3. Balzani, V.; Armaroli, N. *Energy for A Sustainable World: From the Oil Age to a Sun-Powered Future*; John Wiley & Sons: Hoboken, NJ, USA, 2010; p. 390.
4. Adewole, J.K.; Ahmad, A.L.; Ismail, S.; Leo, C.P. Current challenges in membrane separation of CO_2 from natural gas: A review. *Int. J. Greenh. Gas Control* **2013**, *17*, 46–65. [CrossRef]
5. Analysis–Spencer Dale, Group Chief Economist. Available online: https://www.bp.com/en/global/corporate/energy-economics/statistical-review-of-world-energy/natural-gas.html (accessed on 1 August 2018).
6. Bp Statistical Review of World Energy. Available online: https://www.bp.com/content/dam/bp/en/corporate/pdf/energy-economics/statistical-review/bp-stats-review-2018-full-report.pdf (accessed on 1 August 2018).
7. Natural Gas. Available online: https://www.bp.com/en/global/corporate/energy-economics/energy-outlook/demand-by-fuel/natural-gas.html (accessed on 1 August 2018).
8. Faramawy, S.; Zaki, T.; Sakr, A.A.E. Natural gas origin, composition, and processing: A review. *J. Nat. Gas Sci. Eng.* **2016**, *34*, 34–54. [CrossRef]
9. Shimekit, B.; Mukhtar, H. *Natural Gas Purification Technologies–Major Advances for CO_2 Separation and Future Directions*; InTech: London, UK, 2012.
10. Baker, R.W.; Lokhandwala, K. Natural gas processing with membranes: An overview. *Ind. Eng. Chem. Res.* **2008**, *47*, 2109–2121. [CrossRef]

11. Bhide, B.D.; Voskericyan, A.; Stern, S.A. Hybrid processes for the removal of acid gases from natural gas. *J. Membr. Sci.* **1998**, *140*, 27–49. [CrossRef]

12. George, G.; Bhoria, N.; AlHallaq, S.; Abdala, A.; Mittal, V. Polymer membranes for acid gas removal from natural gas. *Sep. Purif. Technol.* **2016**, *158*, 333–356. [CrossRef]

13. Xu, G.; Liang, F.; Yang, Y.; Hu, Y.; Zhang, K.; Liu, W. An improved CO_2 separation and purification system based on cryogenic separation and distillation theory. *Energies* **2014**, *7*, 3484–3502. [CrossRef]

14. Maqsood, K.; Pal, J.; Turunawarasu, D.; Pal, A.J.; Ganguly, S. Performance enhancement and energy reduction using hybrid cryogenic distillation networks for purification of natural gas with high CO_2 content. *Korean J. Chem. Eng.* **2014**, *31*, 1120–1135. [CrossRef]

15. Mandal, B.P.; Guha, M.; Biswas, A.K.; Bandyopadhyay, S.S. Removal of carbon dioxide by absorption in mixed amines: Modelling of absorption in aqueous mdea/mea and amp/mea solutions. *Chem. Eng. Sci.* **2001**, *56*, 6217–6224. [CrossRef]

16. Siriwardane, R.V.; Shen, M.-S.; Fisher, E.P.; Poston, J.A. Adsorption of CO_2 on molecular sieves and activated carbon. *Energy Fuels* **2001**, *15*, 279–284. [CrossRef]

17. Cavenati, S.; Grande, C.A.; Rodrigues, A.E. Removal of carbon dioxide from natural gas by vacuum pressure swing adsorption. *Energy Fuels* **2006**, *20*, 2648–2659. [CrossRef]

18. Peters, L.; Hussain, A.; Follmann, M.; Melin, T.; Hägg, M.B. CO_2 removal from natural gas by employing amine absorption and membrane technology—A technical and economical analysis. *Chem. Eng. J.* **2011**, *172*, 952–960. [CrossRef]

19. Staudt-Bickel, C.; Koros, W.J. Improvement of CO_2/CH_4 separation characteristics of polyimides by chemical crosslinking. *J. Membr. Sci.* **1999**, *155*, 145–154. [CrossRef]

20. Baker, R.W. Future directions of membrane gas separation technology. *Ind. Eng. Chem. Res.* **2002**, *41*, 1393–1411. [CrossRef]

21. Bikson, B.; Nelson, J.K.; Muruganandam, N. Composite cellulose acetate/poly(methyl methacrylate) blend gas separation membranes. *J. Membr. Sci.* **1994**, *94*, 313–328. [CrossRef]

22. Gantzel, P.K.; Merten, U. Gas separations with high-flux cellulose acetate membranes. *Ind. Eng. Chem. Process Des. Dev.* **1970**, *9*, 331–332. [CrossRef]

23. Kim, M.H.; Kim, J.H.; Kim, C.K.; Kang, Y.S.; Park, H.C.; Won, J.O. Control of phase separation behavior of pc/pmma blends and their application to the gas separation membranes. *J. Polym. Sci. Part B Polym. Phys.* **1999**, *37*, 2950–2959. [CrossRef]

24. Şen, D.; Kalıpçılar, H.; Yilmaz, L. Development of polycarbonate based zeolite 4a filled mixed matrix gas separation membranes. *J. Membr. Sci.* **2007**, *303*, 194–203. [CrossRef]

25. Hellums, M.W.; Koros, W.J.; Husk, G.R.; Paul, D.R. Fluorinated polycarbonates for gas separation applications. *J. Membr. Sci.* **1989**, *46*, 93–112. [CrossRef]

26. Lai, J.-Y.; Liu, M.-J.; Lee, K.-R. Polycarbonate membrane prepared via a wet phase inversion method for oxygen enrichment from air. *J. Membr. Sci.* **1994**, *86*, 103–118. [CrossRef]

27. Ward, W.J.; Browall, W.R.; Salemme, R.M. Ultrathin silicone/polycarbonate membranes for gas separation processes. *J. Membr. Sci.* **1976**, *1*, 99–108. [CrossRef]

28. Kesting, R.E.; Fritzsche, A.K.; Murphy, M.K.; Cruse, C.A.; Handermann, A.C.; Malon, R.F.; Moore, M.D. The second-generation polysulfone gas-separation membrane. I. The use of lewis acid: Base complexes as transient templates to increase free volume. *J. Appl. Polym. Sci.* **1990**, *40*, 1557–1574. [CrossRef]

29. Gür, T.M. Permselectivity of zeolite filled polysulfone gas separation membranes. *J. Membr. Sci.* **1994**, *93*, 283–289. [CrossRef]

30. Ahn, J.; Chung, W.-J.; Pinnau, I.; Guiver, M.D. Polysulfone/silica nanoparticle mixed-matrix membranes for gas separation. *J. Membr. Sci.* **2008**, *314*, 123–133. [CrossRef]

31. Hu, C.-C.; Liu, T.-C.; Lee, K.-R.; Ruaan, R.-C.; Lai, J.-Y. Zeolite-filled pmma composite membranes: Influence of coupling agent addition on gas separation properties. *Desalination* **2006**, *193*, 14–24. [CrossRef]

32. Jao-Ming, C.; Da-Ming, W.; Fung-Ching, L.; Juin-Yih, L. Formation and gas flux of asymmetric pmma membranes. *J. Membr. Sci.* **1996**, *109*, 93–107. [CrossRef]

33. Lai, J.-Y.; Huang, S.-J.; Chen, S.-H. Poly(methyl methacrylate)/(dmf/metal salt) complex membrane for gas separation. *J. Membr. Sci.* **1992**, *74*, 71–82. [CrossRef]

34. Budd, P.M.; Elabas, E.S.; Ghanem, B.S.; Makhseed, S.; McKeown, N.B.; Msayib, K.J.; Tattershall, C.E.; Wang, D. Solution-processed, organophilic membrane derived from a polymer of intrinsic microporosity. *Adv. Mater.* **2004**, *16*, 456–459. [CrossRef]

35. Budd, P.M.; Msayib, K.J.; Tattershall, C.E.; Ghanem, B.S.; Reynolds, K.J.; McKeown, N.B.; Fritsch, D. Gas separation membranes from polymers of intrinsic microporosity. *J. Membr. Sci.* **2005**, *251*, 263–269. [CrossRef]

36. Zhang, C.; Yan, J.; Tian, Z.; Liu, X.; Cao, B.; Li, P. Molecular design of tröger's base-based polymers containing spirobichroman structure for gas separation. *Ind. Eng. Chem. Res.* **2017**, *56*, 12783–12788. [CrossRef]

37. Zhang, C.; Fu, L.; Tian, Z.; Cao, B.; Li, P. Post-crosslinking of triptycene-based tröger's base polymers with enhanced natural gas separation performance. *J. Membr. Sci.* **2018**, *556*, 277–284. [CrossRef]

38. Scholes, C.A.; Stevens, G.W.; Kentish, S.E. Membrane gas separation applications in natural gas processing. *Fuel* **2012**, *96*, 15–28. [CrossRef]

39. Liaw, D.-J.; Wang, K.-L.; Huang, Y.-C.; Lee, K.-R.; Lai, J.-Y.; Ha, C.-S. Advanced polyimide materials: Syntheses, physical properties and applications. *Progr. Polym. Sci.* **2012**, *37*, 907–974. [CrossRef]

40. Wang, S.; Li, X.; Wu, H.; Tian, Z.; Xin, Q.; He, G.; Peng, D.; Chen, S.; Yin, Y.; Jiang, Z.; Guiver, M.D. Advances in high permeability polymer-based membrane materials for CO_2 separations. *Energy Environ. Sci.* **2016**, *9*, 1863–1890. [CrossRef]

41. Wind, J.D.; Staudt-Bickel, C.; Paul, D.R.; Koros, W.J. The effects of crosslinking chemistry on CO_2 plasticization of polyimide gas separation membranes. *Ind. Eng. Chem. Res.* **2002**, *41*, 6139–6148. [CrossRef]

42. Swaidan, R.J.; Ma, X.; Litwiller, E.; Pinnau, I. Enhanced propylene/propane separation by thermal annealing of an intrinsically microporous hydroxyl-functionalized polyimide membrane. *J. Membr. Sci.* **2015**, *495*, 235–241. [CrossRef]

43. Staudt-Bickel, C.; Koros, W.J. Olefin/paraffin gas separations with 6fda-based polyimide membranes. *J. Membr. Sci.* **2000**, *170*, 205–214. [CrossRef]

44. Das, M.; Koros, W.J. Performance of 6fda–6fpda polyimide for propylene/propane separations. *J. Membr. Sci.* **2010**, *365*, 399–408. [CrossRef]

45. Krol, J.J.; Boerrigter, M.; Koops, G.H. Polyimide hollow fiber gas separation membranes: Preparation and the suppression of plasticization in propane/propylene environments. *J. Membr. Sci.* **2001**, *184*, 275–286. [CrossRef]

46. Velioğlu, S.; Ahunbay, M.G.; Tantekin-Ersolmaz, S.B. Propylene/propane plasticization in polyimide membranes. *J. Membr. Sci.* **2016**, *501*, 179–190. [CrossRef]

47. Salinas, O.; Ma, X.; Litwiller, E.; Pinnau, I. Ethylene/ethane permeation, diffusion and gas sorption properties of carbon molecular sieve membranes derived from the prototype ladder polymer of intrinsic microporosity (pim-1). *J. Membr. Sci.* **2016**, *504*, 133–140. [CrossRef]

48. Xu, L.; Rungta, M.; Koros, W.J. Matrimid®derived carbon molecular sieve hollow fiber membranes for ethylene/ethane separation. *J. Membr. Sci.* **2011**, *380*, 138–147. [CrossRef]

49. Zhou, S.; Stern, S.A. The effect of plasticization on the transport of gases in and through glassy polymers. *J. Polym. Sci. Part B Polym. Phys.* **1989**, *27*, 205–222. [CrossRef]

50. Tiwari, R.R.; Smith, Z.P.; Lin, H.; Freeman, B.D.; Paul, D.R. Gas permeation in thin films of "high free-volume" glassy perfluoropolymers: Part ii. CO_2 plasticization and sorption. *Polymer* **2015**, *61*, 1–14. [CrossRef]

51. Sanders, E.S. Penetrant-induced plasticization and gas permeation in glassy polymers. *J. Membr. Sci.* **1988**, *37*, 63–80. [CrossRef]

52. Chiou, J.S.; Barlow, J.W.; Paul, D.R. Plasticization of glassy polymers by CO_2. *J. Appl. Polym. Sci.* **1985**, *30*, 2633–2642. [CrossRef]

53. Li, P.; Chung, T.S.; Paul, D.R. Gas sorption and permeation in pim-1. *J. Membr. Sci.* **2013**, *432*, 50–57. [CrossRef]

54. Bos, A.; Pünt, I.G.M.; Wessling, M.; Strathmann, H. CO_2-induced plasticization phenomena in glassy polymers. *J. Membr. Sci.* **1999**, *155*, 67–78. [CrossRef]

55. Petropoulos, J.H. Plasticization effects on the gas permeability and permselectivity of polymer membranes. *J. Membr. Sci.* **1992**, *75*, 47–59. [CrossRef]

56. Kratochvil, A.M.; Koros, W.J. Decarboxylation-induced cross-linking of a polyimide for enhanced CO_2 plasticization resistance. *Macromolecules* **2008**, *41*, 7920–7927. [CrossRef]

57. Qiu, W.; Chen, C.-C.; Xu, L.; Cui, L.; Paul, D.R.; Koros, W.J. Sub-tg cross-linking of a polyimide membrane for enhanced CO_2 plasticization resistance for natural gas separation. *Macromolecules* **2011**, *44*, 6046–6056. [CrossRef]

58. Zhang, C.; Li, P.; Cao, B. Decarboxylation crosslinking of polyimides with high CO_2/CH_4 separation performance and plasticization resistance. *J. Membr. Sci.* **2017**, *528*, 206–216. [CrossRef]

59. Zhang, C.; Cao, B.; Li, P. Thermal oxidative crosslinking of phenolphthalein-based cardo polyimides with enhanced gas permeability and selectivity. *J. Membr. Sci.* **2018**, *546*, 90–99. [CrossRef]

60. Tian, Z.; Cao, B.; Li, P. Effects of sub-tg cross-linking of triptycene-based polyimides on gas permeation, plasticization resistance and physical aging properties. *J. Membr. Sci.* **2018**, *560*, 87–96. [CrossRef]

61. Bos, A.; Pünt, I.G.M.; Wessling, M.; Strathmann, H. Plasticization-resistant glassy polyimide membranes for CO_2/co4 separations. *Sep. Purif. Technol.* **1998**, *14*, 27–39. [CrossRef]

62. Park, H.B.; Jung, C.H.; Lee, Y.M.; Hill, A.J.; Pas, S.J.; Mudie, S.T.; Van Wagner, E.; Freeman, B.D.; Cookson, D.J. Polymers with cavities tuned for fast selective transport of small molecules and ions. *Science* **2007**, *318*, 254–258. [CrossRef]

63. Gleason, K.L.; Smith, Z.P.; Liu, Q.; Paul, D.R.; Freeman, B.D. Pure- and mixed-gas permeation of CO_2 and CH_4 in thermally rearranged polymers based on 3,3′-dihydroxy-4,4′-diamino-biphenyl (hab) and 2,2′-bis-(3,4-dicarboxyphenyl) hexafluoropropane dianhydride (6fda). *J. Membr. Sci.* **2015**, *475*, 204–214. [CrossRef]

64. Shao, L.; Chung, T.; Goh, S.; Pramoda, K. Polyimide modification by a linear aliphatic diamine to enhance transport performance and plasticization resistance. *J. Membr. Sci.* **2005**. [CrossRef]

65. Shao, L.; Chung, T.-S.; Goh, S.H.; Pramoda, K.P. The effects of 1,3-cyclohexanebis(methylamine) modification on gas transport and plasticization resistance of polyimide membranes. *J. Membr. Sci.* **2005**, *267*, 78–89. [CrossRef]

66. Xiao, Y.; Shao, L.; Chung, T.-S.; Schiraldi, D.A. Effects of thermal treatments and dendrimers chemical structures on the properties of highly surface cross-linked polyimide films. *Ind. Eng. Chem. Res.* **2005**, *44*, 3059–3067. [CrossRef]

67. Tin, P.S.; Chung, T.S.; Liu, Y.; Wang, R.; Liu, S.L.; Pramoda, K.P. Effects of cross-linking modification on gas separation performance of matrimid membranes. *J. Membr. Sci.* **2003**, *225*, 77–90. [CrossRef]

68. Wind, J.D.; Sirard, S.M.; Paul, D.R.; Green, P.F.; Johnston, K.P.; Koros, W.J. Carbon dioxide-induced plasticization of polyimide membranes: Pseudo-equilibrium relationships of diffusion, sorption, and swelling. *Macromolecules* **2003**, *36*, 6433–6441. [CrossRef]

69. Wind, J.D.; Staudt-Bickel, C.; Paul, D.R.; Koros, W.J. Solid-state covalent cross-linking of polyimide membranes for carbon dioxide plasticization reduction. *Macromolecules* **2003**, *36*, 1882–1888. [CrossRef]

70. Bos, A.; Pünt, I.G.M.; Wessling, M.; Strathmann, H. Suppression of CO_2-plasticization by semiinterpenetrating polymer network formation. *J. Polym. Sci. Part B Polym. Phys.* **1998**, *36*, 1547–1556. [CrossRef]

71. Maya, E.M.; Sanchez, M.L.; Marcos, A.; de la Campa, J.G.; de Abajo, J. Preparation and properties of catalyzed polyimide/dicyanate semi-interpenetrating networks for polymer gas membrane with suppressed CO_2-plasticization. *J. Appl. Polym. Sci.* **2011**, *124*, 713–722. [CrossRef]

72. Low, B.T.; Chung, T.S.; Chen, H.; Jean, Y.-C.; Pramoda, K.P. Tuning the free volume cavities of polyimide membranes via the construction of pseudo-interpenetrating networks for enhanced gas separation performance. *Macromolecules* **2009**, *42*, 7042–7054. [CrossRef]

73. Kammakakam, I.; Wook Yoon, H.; Nam, S.; Bum Park, H.; Kim, T.-H. Novel piperazinium-mediated crosslinked polyimide membranes for high performance CO_2 separation. *J. Membr. Sci.* **2015**, *487*, 90–98. [CrossRef]

74. Askari, M.; Chung, T.-S. Natural gas purification and olefin/paraffin separation using thermal cross-linkable co-polyimide/zif-8 mixed matrix membranes. *J. Membr. Sci.* **2013**, *444*, 173–183. [CrossRef]

75. Zhuang, G.-L.; Tseng, H.-H.; Uchytil, P.; Wey, M.-Y. Enhancing the CO_2 plasticization resistance of ps mixed-matrix membrane by blunt zeolitic imidazolate framework. *J. CO_2 Utilization* **2018**, *25*, 79–88. [CrossRef]

76. Jusoh, N.; Yeong, Y.F.; Lau, K.K.; Shariff, A.M. Enhanced gas separation performance using mixed matrix membranes containing zeolite t and 6fda-durene polyimide. *J. Membr. Sci.* **2017**, *525*, 175–186. [CrossRef]

77. Shahid, S.; Nijmeijer, K. Performance and plasticization behavior of polymer–mof membranes for gas separation at elevated pressures. *J. Membr. Sci.* **2014**, *470*, 166–177. [CrossRef]

78.　Bachman, J.E.; Long, J.R. Plasticization-resistant ni2(dobdc)/polyimide composite membranes for the removal of CO_2 from natural gas. *Energy Environ. Sci.* **2016**, *9*, 2031–2036. [CrossRef]

79.　Kapantaidakis, G.C.; Kaldis, S.P.; Dabou, X.S.; Sakellaropoulos, G.P. Gas permeation through psf-pi miscible blend membranes. *J. Membr. Sci.* **1996**, *110*, 239–247. [CrossRef]

80.　Bos, A.; Pünt, I.; Strathmann, H.; Wessling, M. Suppression of gas separation membrane plasticization by homogeneous polymer blending. *AIChE J.* **2004**, *47*, 1088–1093. [CrossRef]

81.　Yong, W.F.; Chung, T.-S. Miscible blends of carboxylated polymers of intrinsic microporosity (cpim-1) and matrimid. *Polymer* **2015**, *59*, 290–297. [CrossRef]

82.　Yong, W.F.; Li, F.Y.; Chung, T.S.; Tong, Y.W. Molecular interaction, gas transport properties and plasticization behavior of cpim-1/torlon blend membranes. *J. Membr. Sci.* **2014**, *462*, 119–130. [CrossRef]

83.　Liu, Y.; Wang, R.; Chung, T.-S. Chemical cross-linking modification of polyimide membranes for gas separation. *J. Membr. Sci.* **2001**, *189*, 231–239. [CrossRef]

84.　Shao, L.; Liu, L.; Cheng, S.-X.; Huang, Y.-D.; Ma, J. Comparison of diamino cross-linking in different polyimide solutions and membranes by precipitation observation and gas transport. *J. Membr. Sci.* **2008**, *312*, 174–185. [CrossRef]

85.　Chung, T.-S.; Chng, M.L.; Pramoda, K.P.; Xiao, Y. Pamam dendrimer-induced cross-linking modification of polyimide membranes. *Langmuir* **2004**, *20*, 2966–2969. [CrossRef]

86.　Xiao, Y.; Chung, T.-S.; Chng, M.L. Surface characterization, modification chemistry, and separation performance of polyimide and polyamidoamine dendrimer composite films. *Langmuir* **2004**, *20*, 8230–8238. [CrossRef]

87.　Shao, L.; Chung, T.-S.; Goh, S.H.; Pramoda, K.P. Transport properties of cross-linked polyimide membranes induced by different generations of diaminobutane (dab) dendrimers. *J. Membr. Sci.* **2004**, *238*, 153–163. [CrossRef]

88.　Zhao, H.-Y.; Cao, Y.-M.; Ding, X.-L.; Zhou, M.-Q.; Liu, J.-H.; Yuan, Q. Poly(ethylene oxide) induced cross-linking modification of matrimid membranes for selective separation of CO_2. *J. Membr. Sci.* **2008**, *320*, 179–184. [CrossRef]

89.　Wind, J.D.; Paul, D.R.; Koros, W.J. Natural gas permeation in polyimide membranes. *J. Membr. Sci.* **2004**, *228*, 227–236. [CrossRef]

90.　Park, H.B.; Lee, C.H.; Sohn, J.Y.; Lee, Y.M.; Freeman, B.D.; Kim, H.J. Effect of crosslinked chain length in sulfonated polyimide membranes on water sorption, proton conduction, and methanol permeation properties. *J. Membr. Sci.* **2006**, *285*, 432–443. [CrossRef]

91.　Seo, J.; Jang, W.; Lee, S.; Han, H. The stability of semi-interpenetrating polymer networks based on sulfonated polyimide and poly(ethylene glycol) diacrylate for fuel cell applications. *Polym. Degrad. Stab.* **2008**, *93*, 298–304. [CrossRef]

92.　Alam, S.; Kandpal, L.D.; Varma, I.K. Ethynyl-terminated imide oligomers. *J. Macromol. Sci. Part C* **1993**, *33*, 291–320. [CrossRef]

93.　Alaslai, N.; Ghanem, B.; Alghunaimi, F.; Litwiller, E.; Pinnau, I. Pure- and mixed-gas permeation properties of highly selective and plasticization resistant hydroxyl-diamine-based 6fda polyimides for CO_2/CH_4 separation. *J. Membr. Sci.* **2016**, *505*, 100–107. [CrossRef]

94.　Vinoba, M.; Bhagiyalakshmi, M.; Alqaheem, Y.; Alomair, A.A.; Pérez, A.; Rana, M.S. Recent progress of fillers in mixed matrix membranes for CO_2 separation: A review. *Sep. Purif. Technol.* **2017**, *188*, 431–450. [CrossRef]

95.　Rezakazemi, M.; Ebadi Amooghin, A.; Montazer-Rahmati, M.M.; Ismail, A.F.; Matsuura, T. State-of-the-art membrane based CO_2 separation using mixed matrix membranes (mmms): An overview on current status and future directions. *Progr. Polym. Sci.* **2014**, *39*, 817–861. [CrossRef]

96.　Vu, D.Q.; Koros, W.J.; Miller, S.J. Mixed matrix membranes using carbon molecular sieves: I. Preparation and experimental results. *J. Membr. Sci.* **2003**, *211*, 311–334. [CrossRef]

97.　Singh, A.; Koros, W.J. Significance of entropic selectivity for advanced gas separation membranes. *Ind. Eng. Chem. Res.* **1996**, *35*, 1231–1234. [CrossRef]

98.　Anson, M.; Marchese, J.; Garis, E.; Ochoa, N.; Pagliero, C. Abs copolymer-activated carbon mixed matrix membranes for CO_2/CH_4 separation. *J. Membr. Sci.* **2004**, *243*, 19–28. [CrossRef]

99.　García, M.G.; Marchese, J.; Ochoa, N.A. High activated carbon loading mixed matrix membranes for gas separations. *J. Mater. Sci.* **2012**, *47*, 3064–3075. [CrossRef]

100. Marchese, J.; Anson, M.; Ochoa, N.A.; Prádanos, P.; Palacio, L.; Hernández, A. Morphology and structure of abs membranes filled with two different activated carbons. *Chem. Eng. Sci.* **2006**, *61*, 5448–5454. [CrossRef]

101. Rostamizadeh, M.; Rezakazemi, M.; Shahidi, K.; Mohammadi, T. Gas permeation through h2-selective mixed matrix membranes: Experimental and neural network modeling. *Int. J. Hydrog. Energy* **2013**, *38*, 1128–1135. [CrossRef]

102. Adams, R.T.; Lee, J.S.; Bae, T.-H.; Ward, J.K.; Johnson, J.R.; Jones, C.W.; Nair, S.; Koros, W.J. CO_2–CH_4 permeation in high zeolite 4a loading mixed matrix membranes. *J. Membr. Sci.* **2011**, *367*, 197–203. [CrossRef]

103. Merkel, T.C.; He, Z.; Pinnau, I.; Freeman, B.D.; Meakin, P.; Hill, A.J. Effect of nanoparticles on gas sorption and transport in poly(1-trimethylsilyl-1-propyne). *Macromolecules* **2003**, *36*, 6844–6855. [CrossRef]

104. Ge, L.; Zhou, W.; Rudolph, V.; Zhu, Z. Mixed matrix membranes incorporated with size-reduced cu-btc for improved gas separation. *J. Mater. Chem. A* **2013**, *1*, 6350–6358. [CrossRef]

105. He, Z.; Pinnau, I.; Morisato, A. Nanostructured poly(4-methyl-2-pentyne)/silica hybrid membranes for gas separation. *Desalination* **2002**, *146*, 11–15. [CrossRef]

106. Yang, T.; Chung, T.-S. High performance zif-8/pbi nano-composite membranes for high temperature hydrogen separation consisting of carbon monoxide and water vapor. *Int. J. Hydrog. Energy* **2013**, *38*, 229–239. [CrossRef]

107. Japip, S.; Wang, H.; Xiao, Y.; Shung Chung, T. Highly permeable zeolitic imidazolate framework (zif)-71 nano-particles enhanced polyimide membranes for gas separation. *J. Membr. Sci.* **2014**, *467*, 162–174. [CrossRef]

108. Shahid, S.; Nijmeijer, K. High pressure gas separation performance of mixed-matrix polymer membranes containing mesoporous fe(btc). *J. Membr. Sci.* **2014**, *459*, 33–44. [CrossRef]

109. Caro, J. Are mof membranes better in gas separation than those made of zeolites? *Curr. Opin. Chem. Eng.* **2011**, *1*, 77–83. [CrossRef]

110. Matsui, S.; Ishiguro, T.; Higuchi, A.; Nakagawa, T. Effect of ultraviolet light irradiation on gas permeability in polyimide membranes. 1. Irradiation with low pressure mercury lamp on photosensitive and nonphotosensitive membranes. *J. Polym. Sci. Part B Polym. Phys.* **1998**, *35*, 2259–2269. [CrossRef]

111. Matsui, S.; Nakagawa, T. Effect of ultraviolet light irradiation on gas permeability in polyimide membranes. Ii. Irradiation of membranes with high-pressure mercury lamp. *J. Appl. Polym. Sci.* **1998**, *67*, 49–60. [CrossRef]

112. Hayes, R.A. EI du Pont de Nemours and Co. Polyimide Gas Separation Membranes. U.S. Patent 4,717,393, 1988.

113. Kita, H.; Inada, T.; Tanaka, K.; Okamoto, K.-I. Effect of photocrosslinking on permeability and permselectivity of gases through benzophenone- containing polyimide. *J. Membr. Sci.* **1994**, *87*, 139–147. [CrossRef]

114. Liu, Y.; Pan, C.; Ding, M.; Xu, J. Gas permeability and permselectivity of photochemically crosslinked copolyimides. *J. Appl. Polym. Sci.* **1999**, *73*, 521–526. [CrossRef]

115. Liu, Y.; Pan, C.; Ding, M.; Xu, J. Effect of crosslinking distribution on gas permeability and permselectivity of crosslinked polyimides. *Eur. Polym. J.* **1999**, *35*, 1739–1741. [CrossRef]

116. Kapantaidakis, G.C.; Kaldis, S.P.; Sakellaropoulos, G.P.; Chira, E.; Loppinet, B.; Floudas, G. Interrelation between phase state and gas permeation in polysulfone/polyimide blend membranes. *J. Polym. Sci. Part B Polym. Phys.* **1999**, *37*, 2788–2798. [CrossRef]

117. Hao, L.; Li, P.; Chung, T.-S. Pim-1 as an organic filler to enhance the gas separation performance of ultem polyetherimide. *J. Membr. Sci.* **2014**, *453*, 614–623. [CrossRef]